CO_2 capture in integrated steelworks by commercial-ready technologies and SEWGS process

Matteo Gazzani [a,b], Matteo C. Romano [b,*], Giampaolo Manzolini [b]

[a] *ETH Zurich, Institute of Process Engineering, Sonneggstrasse 3, CH-8092 Zurich, Switzerland*
[b] *Politecnico di Milano, Dipartimento di Energia, Via Lambruschini 4, IT-20156 Milano, Italy*

Received 4 April 2015
Received in revised form 9 July 2015
Accepted 13 July 2015

1. Introduction

Iron and steel industry is the most energy-intensive manufacturing sector accounting for 10-15% of the total industrial primary energy consumption (IPCC, 2005). Being based on fossil fuels and electricity utilization, it accounts for large anthropogenic CO_2 emissions, approximately 5% of the total world emissions (IEA, 2007) (Quader et al., 2015). During the last 15 years, the world crude steel production has experienced a steep increase, reaching 1.6 billion of tonnes per year (World Steel Association, 2014); developing countries like China, India and Brazil played the main role in this sharp growth. Furthermore, the steel demand will very likely rise in the next years along with the urbanization level. Indeed, stabilizing the total CO_2 emissions while increasing the production is a major challenge for the iron and steel industry. In order to mitigate the emissions, two main routes can be pursued: (i) increasing the energy and process efficiency or, (ii) adopting processes for car-bon capture and storage. The former has been effectively fostered during last years: the energy intensity of the steel production has decreased from 25 GJ per tonne of crude steel in 2005 to 20 GJ per tonne in 2012 (World Steel Association, 2013), while the amount of carbon required to reduce the iron in a modern production pro-cess is close to the minimum theoretical value. The corresponding
specific CO_2 emission, which mainly depends on the type of production process, the fuel used and the associated power plant, is
about 1.7 tonne of CO_2 per tonne of crude steel casted (World Steel Association, 2013). It is clear that the resulting amount of emitted tonnes of CO_2 per year is well beyond the limit of a climate-sustainable process and CCS should be effectively deployed in the iron and steel industry.

* Corresponding author. Tel.: +39 0223993846.
E-mail address: matteo.romano@polimi.it (M.C. Romano).

Symbols and Acronyms

BF	blast furnace
BFG	blast furnace gas
BOF	basic oxygen furnace
BOFG	basic oxygen furnace gas
CCR	carbon capture ratio
CCS	carbon capture and storage
CHP	combined heat and power
CO	coke oven
COG	coke oven gas
DCC	direct contact cooler
DRI	direct reduction iron
EBTF	European benchmarking task force
E	CO_2 emissions [kg/s]
e	specific CO_2 emissions [g/kWh]
EAF	electric arc furnace
EBC	environmental barrier coating
GT	gas turbine
HP	high pressure
HR	heat rate
HRSG	heat recovery steam generator
HTS	high temperature shift
IC	inter-cooled
L/G	liquid to gas ratio, weight basis
LHV	low heating value
LP	low pressure
LTS	low temperature shift
$\dot{m}$	mass flow rate [kg/s]
MDEA	methyldiethanolamine
MEA	monoethanolamine
MP	medium pressure
NG	natural gas
NGCC	natural gas combined cycle
p	pressure [bar]
P	electric power [MW]
SC	steam to carbon, [mol/mol]
SEWGS	sorption enhanced water gas shift
SPECCA	specific primary energy consumption for CO_2 avoided, MJ/kg_{CO2}
SRI	smelting reduction iron
T	temperature [°C]
TBC	thermal barrier coating
TGR	top gas recycling
TIT	turbine inlet temperature, [°C or K]
TRL	technology readiness level
WGS	water gas shift

Subscripts

el	electric
f	fuel
Ref	reference
th	thermal

Nowadays, two main steel production routes are followed: the integrated steelworks process and the electric melting-based process. The former route accounts for about 70% of the market share and is by far the production route with the highest specific emissions and the largest emission points. Electric arc furnace (EAF) route accounts for about 28% of the market share. Other processes (e.g., the direct reduction iron (DRI) and the smelting reduction iron (SRI) technologies) have a minor market share, but may gain some advantages over the conventional integrated steelworks process in case of application of CO_2 capture technologies (World Steel Association, 2014).

A simplified configuration of an iron and steel making process in an integrated steelworks is shown in Fig. 1. Following the iron-steel path, iron ore is first reduced to iron metal within the blast furnace (BF) reactor using coke and carbon monoxide originated by coke oxidation as reducing agents. Coke is produced by coal pyrolysis in the coke-oven (CO) plant. The impure iron produced, or pig iron, is manufactured into steel in the basic oxygen furnace (BOF), where the content of carbon and impurities is reduced by blowing oxygen into the liquid metal and by means of additives. Finally, the unfin-ished steel may undergo several downstream processes to get the target steel quality.

Integrated steelworks also includes a power plant, which plays an important role as it consumes the excess process-gas and provides the necessary steam and power to all the key processes. Different plant configurations are adopted for the power generation cycle (Remus et al., 2013). Blast furnace steel mills have been usu-ally integrated with conventional steam cycle power plants, where the steam generated by off-gas combustion is expanded in a steam turbine. The steam generator in such a configuration may also be fed with other fuels like natural gas or oil. The internal steam demand is met by steam turbine bleedings. The relatively simple arrangement can achieve a high level of availability and is designed to use process gases with low calorific value, mainly BFG. However, more efficient combined cycles where low calorific steel mill off-gas is burned in a gas turbine are the preferred solution in modern state-of-the-art plants.

In Fig. 2, the main routes for steel making are schematically shown, indicating the principal material flows and the most attractive gaseous streams where CO_2 capture technologies can be integrated. All the processes involved in integrated steelworks are responsible for a significant portion of the total CO_2 emis-sions, which ultimately result from the combustion of the recycled blended gases. In particular, the following emission points can be identified: (i) the power plant, which accounts for 40–70% of the total CO_2 emissions, (ii) the hot stoves of the blast furnace, 15–30%, (iii) the heating flue of the coke oven plant, 15–20%, (iv) the sinter plant, 5–20% and (v) the lime kiln, 2–5% (Romano et al., 2013).

In an integrated steelworks, the mass and energy interdependency among the different processes is complex because of the many CO and H_2-rich gaseous streams produced by each unit (coke oven gas—COG, blast furnace gas—BFG, and basic oxygen furnace gas—BOFG), which are recycled as fuels in the process. Therefore, several CO_2 capture solutions can be investigated and applied with different levels of integration within the plant. Accordingly, pre-combustion, post-combustion or oxy-combustion CO_2 capture solutions have been proposed. The ULCOS project (ULCOS, 2014) is the most advanced R&D project on CCS application in iron and steel: a shortlist of technologies covering a variety of iron production processes has been identified (Birat, 2008; Helle et al., 2010). Three different capture routes were proposed aiming at reducing the CO_2 produced directly within the ironmaking process: (i) top gas recycling (TGR), which relies on the pure oxygen injection in the BF and the recycle in the BF of the BFG as fuel and reducing agent after CO_2 separation, (ii) Hisarna, a technology based on bath-smelting that combines coal preheating and partial pyrolysis in a separated reactor, and (iii) Ulcored, where CO_2 is captured from the off-gases of a DRI reactor. Being tightly integrated with the iron and steel production process, the proposed concepts require modifications to the plant and process design. Other capture processes integrated with the steel production are reported in (Lampert and Ziebik, 2007) and (Goodman, 2007). The CO_2 removal from blast furnace gases through advanced solvents is proposed in (Dixon et al., 2013). Techno-economic analysis of the most promising technologies for CO_2 capture integrated in the steel plant is reported in

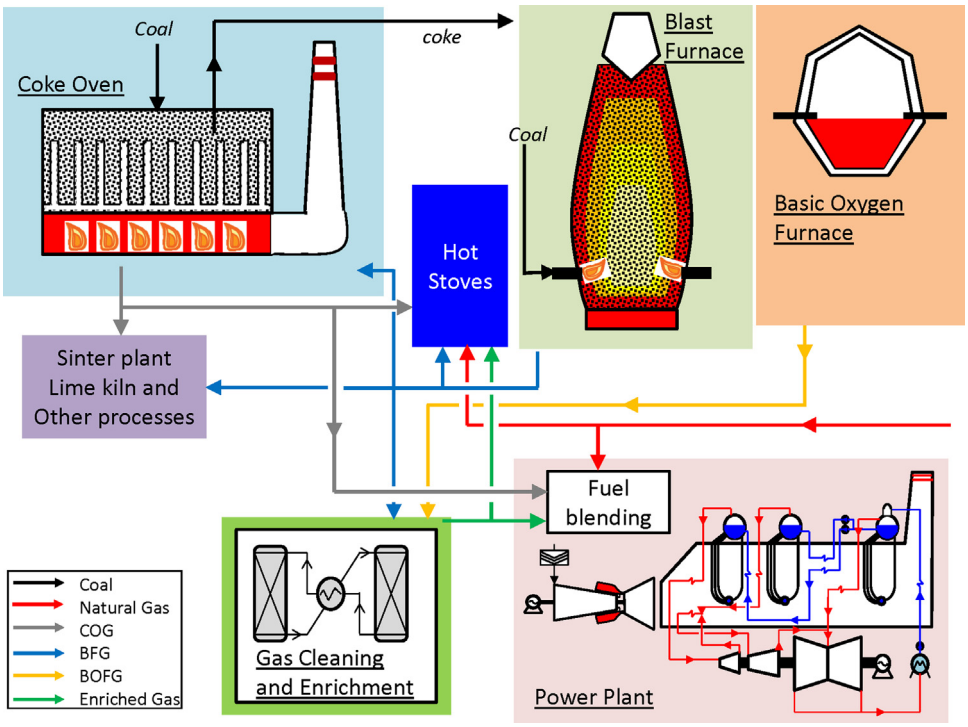

Fig. 1. Simplified layout of an integrated steel mill with combined cycle power plant.

(Ho et al., 2013) and (Kuramochi et al., 2012). An overall review of the state-of-the-art technologies for CO_2 capture in steel making processes is reported in a report from IEAGHG (IEAGHG, 2013). In (Cheng et al., 2010), the potential of capturing CO_2 from the hot stoves flue gas with amines was assessed. The adoption of post-combustion CO_2 capture with amines scrubbing on the power plant and the hot stoves flue gases was studied in (Arasto et al., 2013), who estimated a potential reduction of CO_2 emissions from the entire steel mill of 50% in case of application of a back pressure steam cycle to provide the steam for MEA regeneration, and 75%, in case all the steel mill off-gas is used for steam generation for MEA regeneration, without any electric power production.

One effective strategy to pursuit CO_2 capture in integrated steel mills is the application of the carbon capture process exclusively to the power cycle which uses a large portion of the carbon-rich gases from the iron and steel production units. Accordingly, this solution would potentially cut the CO_2 emissions of the entire steel mill by more than a half, without affecting the steel production

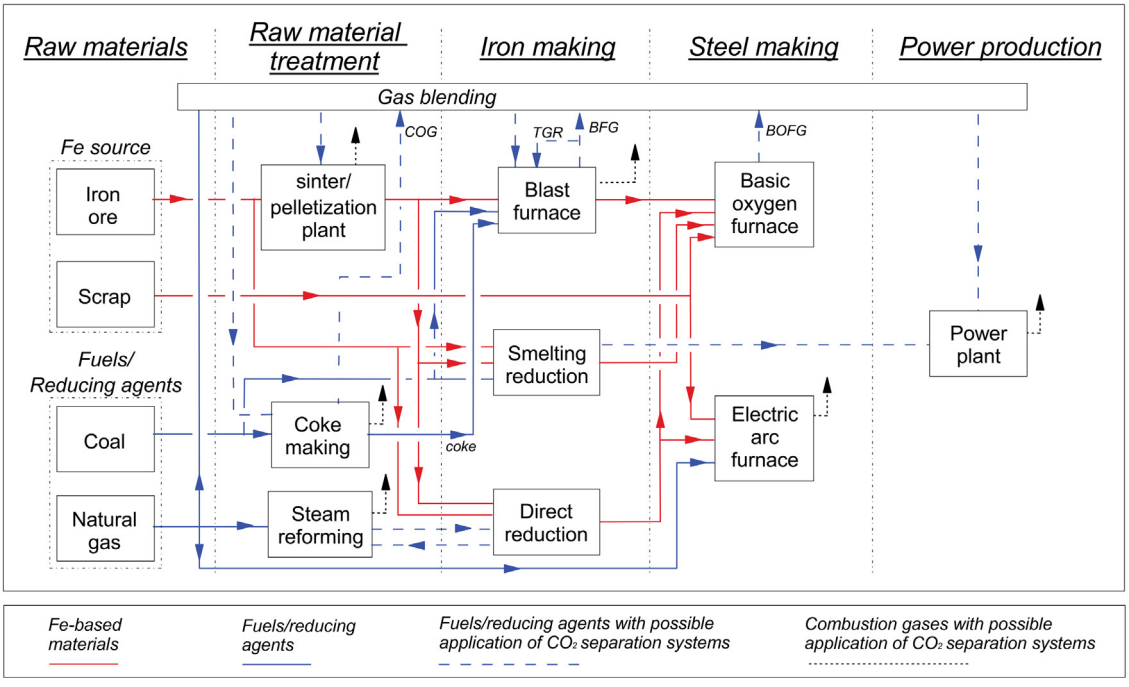

Fig. 2. Strategies and possible applications for CO_2 capture in iron and steel plant.

process and with a significant potential for retrofitting. Moreover, it would open up doors to make use of the know-how developed in the power production field, where extensive research on CCS has long been carried out. On the other hand, it is expected that the potential reduction of CO_2 emissions of more integrated capture configurations such as TGR would be higher than simply acting on the power plant. Ultimately, a comparative economic analysis is necessary to identify the optimal CO_2 capture strategy.

In this paper, both post-combustion and pre-combustion technologies are considered as CO_2 capture systems applied to the power plant. Three different processes are investigated: (i) a benchmark MEA-based post-combustion capture process, (ii) a benchmark MDEA-based pre-combustion capture process and (iii) the innovative pre-combustion process SEWGS (Sorption Enhanced Water Gas Shift), where water gas shift and CO_2 separation are carried out in the same reactor. The MEA and MDEA solutions can be considered commercial-ready and allow benchmarking the plant performance deploying CCS in the iron steel industry nowadays. The SEWGS reactor is a promising second generation concept, mainly developed in the frame of two EU projects (CACHET, 2008; CAESAR, 2010). As discussed in (Romano et al., 2013), SEWGS process appears particularly suitable for application in steelworks power plants, being a pre-combustion capture technology achieving CO_2 separation. Conversely, pre-combustion technologies based on H_2 separation (e.g., hydrogen membranes) are not suitable for this application, as the BFG is highly diluted with nitrogen and hence leading to diluted CO_2 stream after H_2 separation.

This paper presents a thermodynamic analysis of the proposed technologies: different plant configurations are investigated and optimized in order to identify which capture process is more suitable for the steel production operating conditions. Indeed, the thermodynamic analysis should be evaluated along with an economic assessment of the considered plants. Nevertheless, due to the similarities with the power applications and to the unchanged steel island, the economic evaluations developed for electricity gener-ation can be considered a good approximation (Manzolini et al., 2014, 2013a, 2013b; Tsupari et al., 2013).

2. Methodology and assumptions

Mass and energy balances of the overall plants have been estimated using the proprietary code GS, which was developed by the GECoS group of Politecnico di Milano to assess the perfor-mance of gas/steam cycles as well as a variety of other plant options including IGCC, membranes, fuel cells and sorbent-based systems (Campanari, 2000; Campanari et al., 2012; Chiesa and Consonni, 2000; Consonni, 1992; Gazzani et al., 2013c; Macchi et al., 1995; Romano, 2013). The code is conceived for the predic-tion of gas turbine performance at the design point and includes the one-dimensional design of the turbine, functional to calculate the expansion through a stage-by-stage approach, estimating the cooling flows and the evolution of the cooled expansion (Chiesa and Macchi, 2004). Such gas turbine calculation approach is significant for this study where gas turbine is fed with non-conventional fuels and the expansion and blades cooling requirements are calculated taking into account the composition of the combustion gas (Chiesa et al., 2005; Gazzani et al., 2014). Furthermore, GS implements a pinch analysis for the heat recovery steam generator optimization (Lozza, 1990).

Calculations have been performed considering steady state and full load operations of the power plant at design ambient conditions and fuel composition. Though important from the operability and the economics of the power plant, partial load operations as well as changes in the steel gas fuel composition resulting from the modifications of the steel plant production plan have not been considered in this first conceptual work.

2.1. Framework of the gas turbine simulations

Because of the low energy content on volumetric base, the use of steel mill off-gas in gas turbine designed to run on natural gas is challenging. In order to match the operating conditions of the com-pressor and expander while avoiding the onset of surging, the air flow to the combustor must be reduced. This can be achieved either by closing the compressor variable inlet guide vanes, if present, or by reducing the compressor blade height (tip cut). On the other hand, the reduction of the air flow makes the cooling of the com-bustor liner critical so that different modifications to the combustor design are required (Boyce, 2006). Literature and constructor data report that commercially available GT combustors do not require large modifications for LHV value above 2000 kcal/Nm^3 (Alstom Power, 2014; Jones et al., 2011).

In industrial plants, the use low heating value fuels in commercial gas turbines developed for natural gas typically entails the reduction of the firing temperature with respect to the design value of the NG-fired machine. This is performed in order to (i) reduce the degradation of the TBC and the EBC on the high temperature blades due to trace contaminants in the fuel, (ii) reduce the thermal stresses on the GT blades originated by a modification of the heat transfer properties of the expanding gas and of the turbine outlet temperature due to the modified fuel composition and (iii) comply with the maximum power limit of the shaft and the generator (which will increase due to the reduced air flow rate). Nevertheless, following the EBTF approach (Franco et al., 2011), GT simulations are carried out keeping the same technology level of state-of-the-art gas turbines, keeping the key operating parameters (TIT and pressure ratio) unchanged in all the considered plants with respect to the reference NG-fired gas turbine. In other words, it is assumed that the market for the use of CO and H_2-based fuels in high efficiency gas turbines will be sufficiently large for the devel-opment of machines designed for operation with low-BTU fuels, at the same technology level of the corresponding NG-fired machines. Such assumption is consistent with the firing temperature levels reported in (Otsuka et al., 2007) for the use of BFG in MHI F-class turbine.

2.2. CO_2 capture technologies

The absorption-based CO_2 separation processes, i.e. MEA and MDEA, as well as the CO_2 compression have been simulated using ASPEN Plus^{TM} (Manzolini et al., 2011; Romano et al., 2010). The SEWGS process has been extensively simulated during the FP7 CAESAR project for coal and natural gas applications (CAESAR, 2010; Gazzani et al., 2013a, 2013b). A preliminary analysis of the SEWGS application to integrated steel mills is reported in (Gazzani et al., 2013d). Finally, an interesting recent analysis on SEWGS principles is presented in (Boon et al., 2015).

The main calculation assumptions adopted in this work are summarized in Table 1 .

All the investigated plants with carbon capture are compared by means of performance indexes, namely: the net electric efficiency, the CO_2 avoided, and the Specific Primary Energy Consumption for CO_2 Avoided (SPECCA), which measures the primary energy cost related to CO_2 capture. Definitions are shown in Eqs. (1)–(3):

$$\eta_{el} = \frac{P}{\dot{m}_f LHV_f} \quad (1)$$

$$CO_{2\,avoided} = \left(1 - \frac{E}{E_{Ref}}\right) \quad (2)$$

Table 1
Assumptions adopted to simulate the different plant configurations.

Ambient conditions	15 °C/1.013 bar/60% RH
Air composition, dry molar fraction (%)	N_2 78.08%, CO_2 0.04%, Ar 0.93%, O_2 20.95%

Steel mill gases

	N	G	Composition, %							LHV	
	kmol/s	kg/s	H_2	CO	CH_4	C_2H_4	CO_2	N_2	O_2	MJ/kg	MJ/Nm^3
BFG	5.67	174.5	2.42	22.72	0.00	0.18	21.18	53.50	0.00	2.36	3.24
COG	0.47	4.5	60.29	5.04	25.31	3.32	1.29	4.46	0.29	42.73	18.20
BOFG	0.03	0.8	0.96	69.15	0.00	0.09	14.57	14.89	0.34	6.62	8.89
Steel mill off-gas	6.17	180	6.83	21.58	1.93	0.42	19.63	49.58	0.02	3.388	4.41

Temperature 15 °C, Pressure 1.013 bara

Natural gas
Temperature 10 °C, Pressure 70 bar, Molar mass 18.0 kg/kmol
Composition mol% CH_4 89.00, C_2H_6 7.10, C_3H_8 1.00, CO_2 2.00, N_2 0.90 HHV: 51.45 [MJ/kg] LHV 46.48 [MJ/kg]

Gas turbine (generic F class)	
Pressure ratio	18.1
Fuel injection pressure	p_{air} + 10 bar
TIT	1360 °C
Pressure loss in the air filter	1 kPa
Generator efficiency	98.5%
Mechanical efficiency	99.6%
Steam cycle	
Pressure levels	130, 28, 4 bar
Pressure loss, $\Delta p/p$ (SH/RH/ECO)	7/18/25%
Maximum temperature SH e RH	565 °C
Pinch, subcooling, approach ΔT	10/5/25 °C
Condensing pressure	0.048 bar (32 °C)
Turbine isentropic efficiency (HP/IP/LP)	92/94/88%
Pumps efficiency (HP/MP)	82/75%
HRSG thermal losses	0.7% of heat exchanged
HRSG pressure losses, gas side	3 kPa
Power for heat rejection	0.8% of the released heat
Steel gas compressor	
Compressor ratio	28
Number of intercoolers	No capture and MEA: 3; MDEA: 2; SEWGS: 2 or 3
Polytropic efficiency*	88.4–89.3%
Mechanical efficiency	99.8%
MEA CO_2 absorption process	
MEA/water content in the lean solution	30/70%wt
Lean solution CO_2 loading**	0.18 mol-CO_2/mol-MEA
Booster fan pressure ratio	1.1
Booster fan isentropic and driver efficiency	85/95%
Absorber number of ideal stages	4
Stripper number of ideal stages	9
Stripper pressure	1.8 bar
Steam pressure for the stripper reboiler	4.0 bar
Steam temperature entering the reboiler	154 °C
Pinch point ΔT in regenerative heat exchanger	10 °C
Pumps hydraulic/mech.-electric efficiency	75/95%
Water gas shift reactors	
HTS inlet temperature	320 °C
LTS inlet temperature	190 °C
MDEA CO_2 absorption process	
MDEA/water content in the lean solution	40/60%wt.
Lean solution CO_2 loading	0.005 mol-CO_2/mol-MDEA
HP/LP flash pressure	5/1.1 bar
Recycle compressor isentropic/mech.-electric efficiency	80/95%
Stripper number of ideal stages	5
Stripper pressure	1.3 bar
Steam pressure for the stripper reboiler	4.0 bar
Steam temperature entering the reboiler	154 °C
Pinch point regenerative heat exchanger	10 °C
Pumps hydraulic/mech.-electric efficiency	75/95%
*SEWGS process***	
Rinse steam pressure	28 bar
Purge steam pressure	1.1 bar
Rinse/purge steam temperature	400 °C
CO_2 purity	99% mol.

Table 1 (*continued*)

H_2O/CO_2 SEWGS off-gas expander	
Discharge pressure	0.5 bar
Polytropic efficiency	82%
Mechanical efficiency	98.7%
Generator efficiency	98.0%
CO_2 compression	
Final delivery pressure	110 bar
Compressor isentropic efficiency	85%
Temperature for CO_2 liquefaction	25 °C
Mechanical-electrical efficiency	95%
Intercooler outlet temperature	30 °C
Pressure loss, $\Delta p/p$, for each intercooler	1%

* The polytropic efficiency is calculated as function of the machine size parameter.
** Design value of the lean solution loading, not attained in the reference MEA cases due to the shortage of steam.
*** Other assumptions for the SEWGS process are subject to sensitivity analysis and are reported in Section 3.4.

$$\text{SPECCA} = \frac{\text{HR-HR}_{\text{Ref}}}{e_{\text{Ref}} - e} = \frac{36\left(1/\eta - 1/\eta_{\text{Ref}}\right)}{e_{\text{Ref}} - e} \quad (3)$$

Where:

- η_{el} is the net electric efficiency
- P is the net power output [MW]
- $\dot{m}_f$ is the fuel mass flowrate [kg/s]
- LHV_f is the fuel low heating value [MJ/kg_{fuel}]
- HR is the heat rate of the plant, [kJ_{LHV}/kWh_{el}]
- e is the specific CO_2 emission rate, [kg_{CO2}/MWh_{el}]
- Ref indicates the reference case for electricity production without carbon capture, which is the one presented in Section 3.1.

It has to be remarked that the CO_2 avoided index used in this work refers just to the specific emissions from the considered plant and cannot be intended as a full chain, life cycle analysis indicator which should also consider emissions associated to fuel production, transportation and to the electricity exchanged with the electric grid. In particular, the plants assessed in this work are characterized by different power outputs. This has an impact in a life cycle approach, since lower power outputs with respect to the reference case would imply indirect CO_2 emission from a conventional power plant to balance the reduced electric power produced. On one hand, such life cycle approach would provide a comprehensive indication of the real CO_2 avoided by the different capture processes. On the other hand, the results would be highly dependent on the energy mix of the country where the analysis is conducted, which would reduce the generality of the results. For this reason, as normally done in the comparison of CO_2 capture technologies, a gate-to-gate approach has been assumed here instead of a cradle-to-grave one.

3. Description of the power plant configurations

Different plant solutions were investigated integrating the considered technologies, hence determining four main categories: (i) reference case with no capture, (ii) post-combustion MEA-based CO_2 capture, (iii) pre-combustion MDEA-based CO_2 capture and (iv) pre-combustion SEWGS-based CO_2 capture.

In the state-of-the-art iron making plants with combined cycle power stations, steel mill off-gases are often blended with high LHV fuels such as natural gas – when the connection to the grid is available – in order to avoid expensive GT design modifications and to increase the plant electric efficiency and availability. Accordingly, two reference cases without CO_2 capture are proposed in this work: in the first reference case (REF_{withNG}), the power input to the single GT is supplied by both the steel off-gas and the natural gas, contributing respectively by 47.1% and 52.9% of the total heat input on LHV basis (the exact share of the thermal power input corresponds to an existing integrated steel plant). In order to have a realistic size of the gas turbine (F-class), half of the available steel mill syngas is used in this case, i.e., 90 kg/s. In the second reference case ($REF_{w/oNG}$), no natural gas blending is considered and the GT runs exclusively with the steel mill off-gas available at the integrated steelworks battery limit (i.e., 180 kg/s).

Among the CO_2 capture technologies investigated, the MEA process, which is a post-combustion solution and does not require the fuel decarbonization, was simulated for both cases with and without natural gas addition. On the other hand, the pre-combustion cases (MDEA and SEWGS) are based exclusively on steel mill syngas as the use of natural gas would require the adoption of a natural gas reforming system, substantially complicating the process, for a significant overall CO_2 emission reduction.

For the sake of consistency, all plants adopt one GT coupled with one HRSG and one steam turbine. In the cases with natu-ral gas blending the additional heat input would allow the use of two identical GTs fed with the same fuel mixture. In these cases, plants configuration with a single larger steam turbine collecting the steam produced in the two parallel HRSGs would probably be used. A somewhat higher steam turbine efficiency would result in this case, since the larger steam flow rate expanded would lead to larger and more efficient stages. Apart from this effect, not predictable with the EBTF guidelines (Franco et al., 2011), which consider fixed steam turbine sections efficiencies, the performance of the plants are perfectly scalable.

Finally, the steel plant off-gas cleaning is assumed to be performed inside the steel plant battery limit and has not been simulated in this work.

The two reference cases are discussed in the next section. The MEA case is discussed in Section 3.2 while the MDEA and SEWGS pre-combustion plants are described in Sections 3.3 and 3.4 respectively. In Section 4, improved solutions for MEA-based plants and a sensitivity analysis on the SEWGS process parameters are further discussed.

3.1. Reference NGCC plant without capture

In order to develop a state-of-the-art combined cycle interconnected to the steel plant, the assumptions presented by EBTF were chosen as reference (Franco et al., 2011). Starting from the conventional stand-alone combined cycle presented in (Manzolini et al., 2011) the plant was adapted to the iron and steel application. As the steel mill off-gas is released at ambient pressure, the main plant modifications concern the pressurization of the GT fuel. Similarly to the layout proposed in (Otsuka et al., 2007), the power island configuration is a single shaft type which consists of a gas turbine, a generator and a fuel gas compressor connected through a step-up gear device located on the same shaft. The steam turbine could be as well mounted on the same shaft but in this work a conservative, stand-alone steam turbine has been chosen.

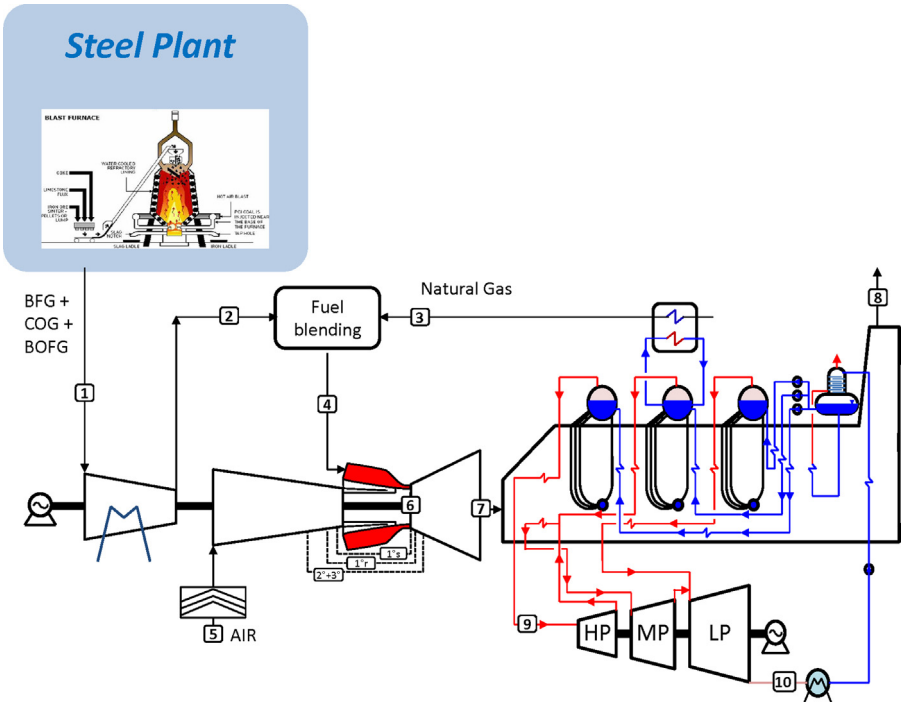

Fig. 3. Layout of the reference no capture combined cycle plant coupled with the integrated steelworks and natural gas addition.

A three-stage intercooled compressor is used for BFG compression. The power required to compress the steel off-gas up to the GT injection pressure represents the largest penalty compared to the stand-alone NG-fuelled combined cycle. Its negative effect is hence proportional to the portion of steel mill off-gas with respect to the total heat input. In the reference case with natural gas dilution, the IC compressor requires about 34 MW to compress 90 kg/s of steel off-gas while in the reference, pure syngas, case the IC compression power doubles to about 67 MW.

Natural gas is preheated to 160 °C by saturated water from the MP drum before blending, while the steel mill off-gas is preheated in the compression process to about 115 °C. No steam supply from the power plant to the integrated steel mill has been considered in this work. Indeed, in most of the integrated steelworks part of the steam generated in the power plant is used in the steel island in a combined heat and power (CHP) configuration. Nevertheless, given that the amount of process steam largely depends on the specific features of the steel island (e.g., final quality and type of steel produced, type of coal adopted), it has been decided to investigate the CCS solutions without penalizing a priori one specific technology. As a matter of fact, large process steam requirements would reduce the capture capability of a steam-intensive technology like MEA. In case a CHP configuration is adopted in the plant, it has to be considered that the CO_2 capture efficiency reported in this work would be affected for the MEA plant and might be affected for the MDEA and SEWGS plants, based on the flow rate of additional steam export, which is very case-specific.

The resulting plant layout for the reference case with NG addition is shown in Fig. 3 while mass balances and overall performance are reported in Table 2. The condensing pressure is set at 0.048 bar assuming the use of a cooling tower. The resulting net power out-put is 316.9 MW with a net electric efficiency of 54.9% and specific CO_2 emission of 851 g/kWh. A state-of-the-art NG fired combined cycle achieves 58.3% of electric efficiency with 352 g/kWh$_{el}$ emis-sion (Franco et al., 2011). The significantly higher emissions are due to the high carbon content and low heating value of the steel plant gases.

Considering the reference case without natural gas dilution, the higher power consumption to compress the steel mill off-gas reduces significantly the efficiency down to 52.3%, with a net electric production of 318.8 MW and CO_2 specific emission equal to 1339 g/kWh$_{el}$. The performance of this cycle is close to the 51.2% efficiency reported in literature for an existing BFG-fired combined cycle based on an F-class gas turbine (Otsuka et al., 2007).

Table 2
Mass flow, temperature, pressure and composition for the integrated steel plant without capture showed in Fig.3.

Stream	$\dot{m}$ (kg/s)	T (°C)	p (bar)	Composition (%mol.)							
				$CH_4 + C_2H_4$	CO	CO_2	H_2	H_2O	Ar	N_2	O_2
1	90.0	15.0	1.01	Steel Plant gas as reported in Table 1							
2	90.0	114.7	27.00								
3	5.9	160.0	70.00	Natural Gas as reported in Table 1							
4	95.9	120.4	27.00	10.35	19.27	17.90	6.53	–	–	44.91	0.02
5	430.0	15.0	1.01	–	–	0.04	–	1.03	0.92	77.28	20.73
6	416.3	1451.1	17.61	–	–	12.08	–	8.15	0.73	71.76	7.29
7	525.8	612.9	1.04	–	–	9.59	–	6.68	0.77	72.90	10.07
8	525.8	80.0	1.01	–	–	9.59	–	6.68	0.77	72.90	10.07
9	61.7	559.5	120.90	–	–	–	–	100.0	–	–	–
10	80.6	32.2	0.048	–	–	–	–	100.0	–	–	–
Net power output: 316.9 MW				**Net electric efficiency: 54.95%**					**CO_2 emissions: 851 g/kWh$_{el}$**		

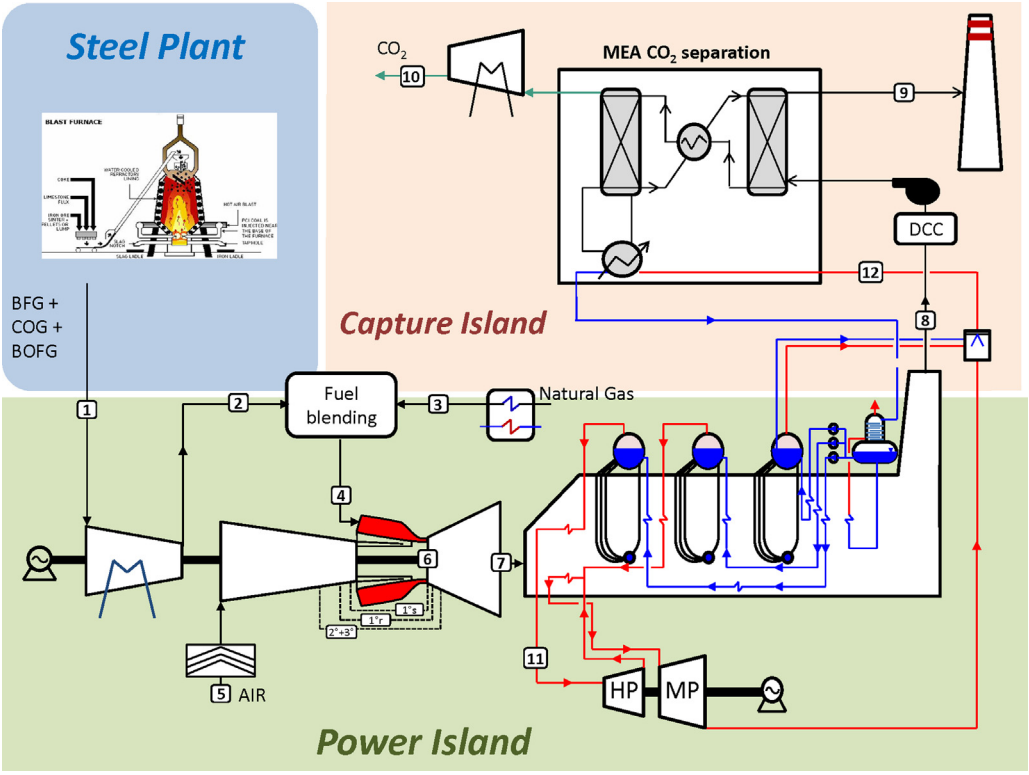

Fig. 4. Plant layout for post-combustion CO_2 capture in an integrated steelworks using the MEA process.

3.2. *Post-combustion capture with MEA*

The MEA process is regarded as the commercial-ready solution for CO_2 capture. Therefore, the first capture plant presented is based on the amine post-combustion process. As mentioned above, the amine scrubbing plant has been simulated considering two different fuels: in MEA_{withNG}, the GT is fuelled with a blending of natural gas and steel mill syngas whilst in $MEA_{w/oNG}$, the GT is fuelled exclusively with the steel mill syngas.

Fig. 4 shows the plant layout: following the power island, which coincides with the reference case, the HRSG exhaust gas is cooled down in a direct contact cooler (DCC) to 40 °C and then fed to the absorber. The additional pressure losses introduced by the MEA process require the adoption of a fan downstream the DCC. The CO_2-free flue gas exiting the absorber is sent to the stack, while almost pure CO_2 is recovered in the desorber, dried and compressed for storage. The MEA process also requires the adoption of a regenerative heat exchanger and several pumps. The heat required for the CO_2 desorption in the reboiler is supplied by LP steam from the steam turbine which is attemperated to about 155 °C by inject-ing saturated water from the LP drum. Mass balance and overall performance of the MEA plant are shown in Table 3.

The CO_2 capture section is simulated with ASPEN Plus® adopting the Rad-Frac equilibrium model and the ENRTL thermodynamic framework. The process consumptions and capture level have been optimized varying the Liquid-to-Gas (L/G) ratio for different flue gas flow rates. Compared to conventional fossil fuel-based power plants, the higher CO_2 content in the exhaust gas slightly reduces the specific heat duty for MEA regeneration to about 3.6 MJ/kg_{CO_2} (vs. 3.96 MJ/kg_{CO_2} of the NG-fired combined cycle and 3.73 MJ/kg_{CO_2} of a PC steam cycle calculated with the same model (Franco et al., 2011)), with an optimized L/G equal to 2.3.

The energy consumption is consistent with similar analyses presented in (Arasto et al., 2013) and (Tobiesen et al., 2011). However, results in term of CO_2 capture and steam consumption differ significantly from the conventional power application: because of the

Table 3
Mass flow, temperature, pressure and composition for the MEA plant with NG addition (MEA with NG). Numbers refer to Fig.4.

Stream	$\dot{m}$ (kg/s)	T (°C)	p (bar)	Composition (%mol.)							
				$CH_4 + C_2H_4$	CO	CO_2	H_2	H_2O	Ar	N_2	O_2
1	90.0	15.0	1.01	Steel Plant gas as reported in Table 1							
2	90.0	114.7	27.00								
3	5.9	160.0	70.00	Natural Gas as reported in Table 1							
4	95.9	120.4	27.00	10.35	19.27	17.90	6.53			44.91	0.02
5	430.0	15.0	1.01	–	–	0.04	–	1.03	0.92	77.28	20.73
6	416.3	1451.1	17.61	–	–	12.08	–	8.15	0.73	71.76	7.29
7	525.8	612.9	1.04	–	–	9.59	–	6.68	0.77	72.90	10.07
8	525.8	142.2	1.01	–	–	9.59	–	6.68	0.77	72.90	10.07
9	492.3	51.8	1.01	–	–	2.47	–	13.32	0.77	73.07	10.16
10	56.0	35.0	1.50	–	–	98.58	–	1.39	0.02	0.01	–
11	61.5	559.5	120.90	–	–	–	–	100	–	–	–
12	92.2	154.0	4.00	–	–	–	–	100	–	–	–
Net power output: 239.5 MW				**Net electric efficiency: 41.53%**				**CO_2 emissions: 292 g/kWh_{el}**			

large CO_2 amount in the steel off-gas, the steam produced in the HRSG is not sufficient to reach high carbon capture values even with the adoption of a back pressure turbine configuration (i.e., all the steam available is condensed in the MEA stripper reboiler).

The resulting net power output of the MEA_{withNG} plant is 239.5 MW with a net electric efficiency of 41.5% and CO_2 emissions of 292 g/kWh$_{el}$, which corresponds to CO_2 avoided of about 66%. On the other hand, in absence of blending with NG, the net power output of the $MEA_{w/oNG}$ plant is 235.7 MW, with a net electric efficiency of 38.7% and CO_2 emissions of 871 g/kWh$_{el}$, which corresponds to CO_2 avoided of about 35%.

3.3. *Pre-combustion capture with MDEA*

CO_2 pre-combustion capture requires several plant modifications compared to the MEA post-combustion case. Thanks to the CO_2 separation, the decarbonized syngas is enriched in hydrogen with a remarkable increase in the weight-based LHV (from 3.39 to 4.97 MJ/kg). As for the second reference case without CO_2 capture, no natural gas addition is considered for the pre-combustion solutions. The main components which must be adopted to decarbonize the steel mill off-gas through an MDEA process are: (i) two Water Gas Shift reactors (WGS) that convert CO into CO_2 and H_2, (ii) the MDEA CO_2 separation unit, (iii) a saturator to humidify the syngas thus reducing the amount of steam bled from the turbine to reach the desired Steam-to-Carbon (S/C) ratio for the WGS reaction and, (iv) several heat exchangers for the thermal integration of the process.

Fig. 5 shows the resulting plant layout. After the intercooled compression, here achieved in two intercooled stages to take advantage from the higher water temperature in the following saturation process, the steel gas is firstly saturated in a saturator using hot water from the compressor intercoolers. It is then mixed with additional steam to reach a steam-to-carbon ratio S/C = 1, heated up to 320 °C in a regenerative heat exchanger and finally sent to the High Temperature Shift (HTS) reactor, where chemical equilibrium is achieved at an outlet temperature of 450 °C. Given that the amount of CO_2 in the flue gas is about 50%vol, S/C = 1 corresponds to S/CO = 1.9, which is in line with the operating conditions of a conventional water gas shift reactor for natural gas or coal gasification derived syngas. The amount of CO converted in the HTS is about 80% while the CO-to-carbon (carbon as CO + CO_2) ratio at the HTS outlet is 10%vol. The heat released by the WGS reaction is recovered producing HP steam in a dedicated waste heat boiler. The second WGS reactor operates at a lower outlet temperature (around 230 °C), thus promoting the CO conversion. The resulting syngas is cooled to ambient temperature and sent to the MDEA pro-cess where a decarbonized GT fuel (H_2 and N_2 with some traces of CH_4, CO and H_2O) and a CO_2 rich stream are produced.

The MDEA process is based on Di-Ethanol Amine partial ther-mal regeneration in a stripper with low pressure steam and partial physical regeneration in a low pressure flash, like in the BASF MDEA process (Kohl and Nielsen, 1997; Meissner and Wagner, 1983; Romano et al., 2010). Rich solution exiting the absorber is first sent to a high pressure flash where most of the hydrogen, carbon monoxide and nitrogen are desorbed and recycled back to the absorber. Afterwards, it enters a low pressure flash where it is partially regenerated. The semi-lean solution exiting the LP flash is partly sent back to the absorber and partly further regenerated in a stripper, where carbon dioxide is stripped with the steam generated in a reboiler. A low pressure steam flow extracted from the steam turbine is condensed in the reboiler to supply the required heat. The lean solvent from the stripper bottom is cooled and sent to the absorber. The vapor flow exiting the stripper, mainly composed

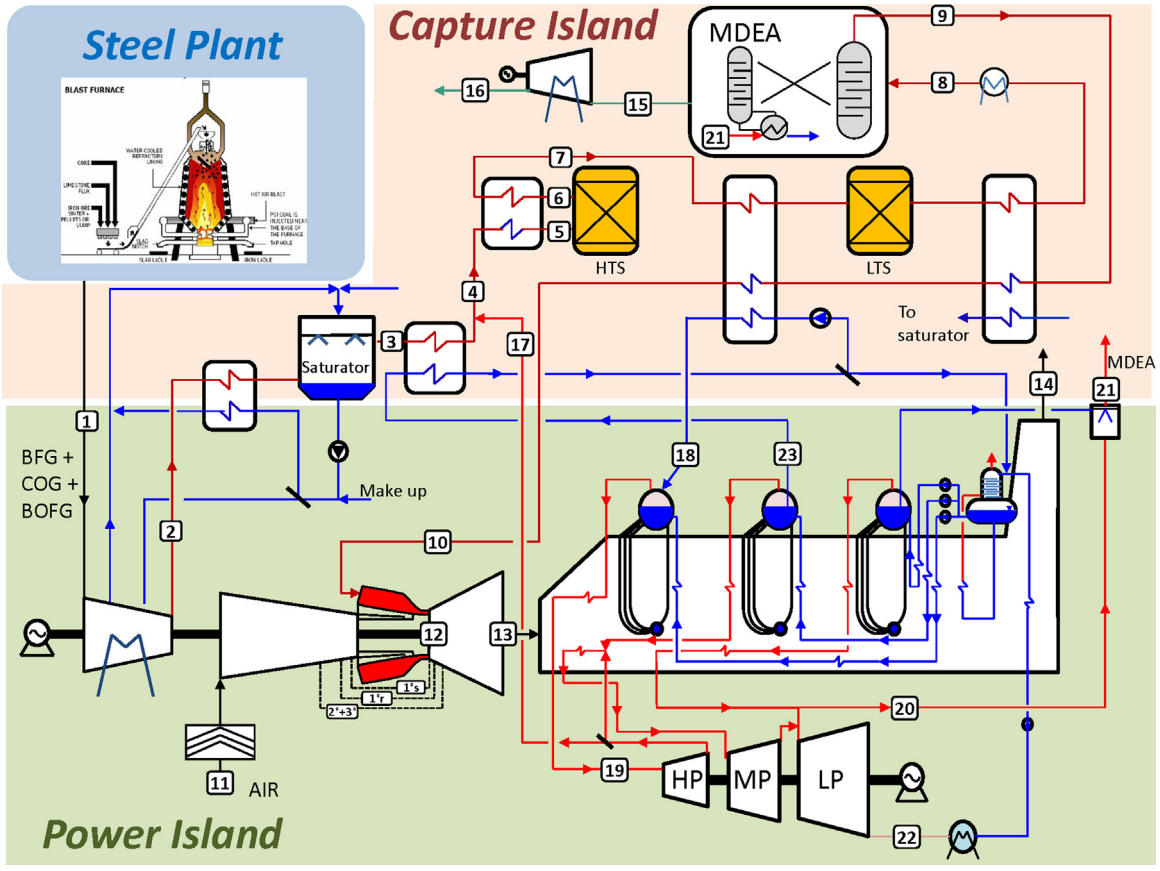

Fig. 5. Plant layout for pre-combustion CO_2 capture in an integrated steelworks using the MDEA process.

Table 4
Mass flow, temperature, pressure and composition for the MDEA plant. Numbers refer to Fig.5.

Stream	$\dot{m}$ (kg/s)	T (°C)	p (bar)	Composition (%mol.)							
				$CH_4 + C_2H_4$	CO	CO_2	H_2	H_2O	Ar	N_2	O_2
1	180.0	30.0	1.01	Steel plant gas as reported in Table 1							
2	180.0	220.3	28.30								
3	212.1	160.5	28.05	1.85	16.53	15.20	5.61	22.33	–	38.49	–
4	225.2	200.0	28.02	1.69	15.16	13.93	5.14	28.80	–	35.28	–
5	225.2	320.0	28.00	1.69	15.16	13.93	5.14	28.80	–	35.28	–
6	225.2	451.0	27.46	1.69	3.36	25.72	16.91	17.03	–	35.28	–
7	225.2	345.5	27.44	1.69	3.36	25.72	16.91	17.03	–	35.28	–
8	203.6	35.0	26.90	1.97	0.35	33.40	23.17	0.21	–	40.91	–
9	93.2	35.2	26.90	2.95	0.52	0.01	34.79	0.31	–	61.42	–
10	93.2	300.0	26.90	2.95	0.52	0.01	34.79	0.31	–	61.42	–
11	375.0	15.0	1.01	–	–	0.04	–	1.03	0.92	77.28	20.73
12	371.4	1461.4	17.60	–	–	1.31	–	14.58	0.67	76.53	6.91
13	489.8	600.7	1.04	–	–	1.05	–	11.76	0.72	76.69	9.78
14	489.8	108.3	1.01	–	–	1.05	–	11.76	0.72	76.69	9.78
15	110.4	35.0	26.70	–	–	96.06	0.01	3.92	–	0.01	–
16	110.4	35.0	110.00	–	–	99.98	0.01	–	–	0.01	–
17	13.1	338.1	28.10	–	–	–	–	100	–	–	–
18	6.4	340.0	132.30	–	–	–	–	100	–	–	–
19	66.5	559.5	120.90	–	–	–	–	100	–	–	–
20	48.4	217.3	4.00	–	–	–	–	100	–	–	–
21	6.7	143.6	4.00	–	–	–	–	100	–	–	–
22	11.8	32.2	0.048	–	–	–	–	100	–	–	–
23	40.3	230.0	28.00	–	–	–	–	100	–	–	–
Net power output: 211.1 MW				**Net electric efficiency: 34.64%**					**CO_2 emissions: 147.1 g/kWh$_{el}$**		

of carbon dioxide and steam, is sent to the LP flash where water condenses providing heat to the rich solution and enhancing semi-lean solvent regeneration. Considering the two regeneration levels attained in the process, the CO_2 absorber is fed with the lean solution at the top of the column and with the semi-lean solution at an intermediate stage (whose position was optimized in the simulations). Accordingly, the energy consumptions of this MDEA process are: (i) steam usage for reboiler, (ii) compression work for syngas recycle and solvent pumping and (iii) heat rejection to the environment from regenerated solvent cooler and LP flash CO_2/H_2O vapor cooling. In this case, thanks to the lower heat for solvent regeneration (1.1 MJ/kg$_{CO_2}$), steam flowing in the steam turbine is enough to feed the stripper reboiler with an extraction and condensing steam turbine, attaining a good solvent regeneration and a high CO_2 capture efficiency.

Concerning the H_2-rich syngas combustion, in order to limit the NO_x production below 20 ppm in a diffusive flame combustor, which represents the state-of-the-art for hydrogen combustion in a GT, the stoichiometric flame temperature must be kept below 2200 K (Gazzani et al., 2014). In IGCC plants, this is achieved by diluting the H_2-rich syngas either with steam or nitrogen. Nevertheless, the steel mill off-gas already contains 50%vol N_2 due to the air used in the blast furnace and the resulting stoichiometric flame temperature is 2170 K. Accordingly, no further dilution is required. This consideration applies to the MDEA as well as the SEWGS plants.

Heat and mass balances of the overall MDEA plant are reported in Table 4. The resulting net power output is 211.1 MW with a net electric efficiency of 34.6% and CO_2 emissions of 147.1 g/kWh$_{el}$, which corresponds to CO_2 avoided of about 89%.

3.4. Pre-combustion capture with SEWGS

The SEWGS process combines the high temperature water gas shift reaction with the adsorption of CO_2 on a solid sorbent. Similarly to Pressure Swing Adsorption (PSA), it comprises of multiple fixed beds operating in parallel that adsorb CO_2 at high temperature and pressure, and release it at low pressure. The combination of CO_2 conversion and removal enhances the H_2 production and the purity of the stream feeding the Gas Turbine (GT) combustor, whilst a separate CO_2 by-product can be recovered from the adsorbent by regenerating the bed. The advantages of combining water gas shift reaction with separation of CO_2 are: (i) high hydrogen and CO_2 recovery: almost all the CO is converted and hydrogen recovery is maximized, (ii) better heat integration: CO_2 is captured at high temperature avoiding temperature swings and, (iii) lower medium pressure steam consumption for the WGS reaction thanks to the CO_2 product subtraction. More information about SEWGS principles are reported in literature and hence only a brief process description is reported here (Allam et al., 2005; Boon et al., 2014; Gazzani et al., 2013b).

Similarly to a common PSA, the SEWGS process is based on the preferential adsorption of one species on solid sorbent. Dur-ing the feed step, syngas flows at high pressure and temperature through the reactor where CO_2 is captured while a hydrogen-rich stream is produced. When the CO_2 front reaches the bed outlet, the feed gas is directed to another vessel while regeneration starts in the current vessel. The first regeneration step is the rinse, where steam pushes the hydrogen-rich gaseous phase out of the reac-tor. After rinsing, the vessel undergoes a depressurization phase to ambient pressure and a purge phase, where the CO_2 product is collected. The final step of the process consists of vessel re-pressurization, firstly through conventional pressure equalization steps and finally receiving counter-current product gas. While the rinse step is responsible for the CO_2 purity level and H_2 recovery, the purge determines the CO_2 capture ratio. As shown in (Wright et al., 2008) and (Van Selow et al., 2008), steam is the most suitable fluid for both bed rinse and purge. Accordingly, most of the energy consumption required by the SEWGS process is due to the steam usage during purge and rinse.

In this work, two different sorbents have been considered, named for simplicity *Sorbent* α and *Sorbent* β; both are potassium carbonate hydrotalcite-based material (Van Selow et al., 2011). The former was tested under thousands of cycles in the multicolumn facility at ECN (NL) during the collaborative EU FP7 projects CACHET (CACHET, 2008) and CAESAR (CAESAR, 2010) while the latter is a new sorbent with improved adsorption capacity (about 100% higher than *sorbent* α) developed and tested at the end of CAESAR. The amounts of steam for SEWGS rinsing and purging adopted in this work are derived from CAESAR results and are shown in Table 5. The different cases reported in this table refer

Table 5
SEWGS data investigated in the sensitivity analysis: steam consumption for rinse and purge as function of the design parameters (sorbent type, target CCR, reactor and train number and overall cycle time). Other process parameters have been kept constant in all the cases as indicated in Table 1 Additional cases are ideally possible but unlikely competitive because of the high steam requirements.

Sorbent type	α								β		
CASE	1	2	3	4	5	6	7	8	9	10	11
CCR* SEWGS	90	90	95	95	95	95	90	95	95	98	98
Reactor-train number	6–9	6–9	6–9	6–9	6–9	6–9	5–9	5–9	5–9	5–9	5–9
Bed length (ft)	44	44	44	22	28	34	28	28	34	28	34
Cycle time (s)	150	180	150	150	180	180	150	150	180	150	150
S/C rinse**	0.52	0.38	0.52	0.22	0.20	0.25	0.22	0.23	0.21	0.24	0.29
S/C purge**	0.56	0.76	0.89	0.60	0.26	0.08	0.25	0.45	0.24	0.73	0.31

* SEWGS CCR is defined as the molar ratio between the $CO + CO_2$ captured and the $CO + CO_2$ entering the reactor
** Steam to carbon values are presented in terms of kmoles of steam per kmoles of total carbon ($CO + CO_2$) in the feed

to different target carbon capture rates, bed length and cycle time, leading to the different *S/C* values tested in this work.

Similarly to the MDEA plant layout, also the SEWGS integration requires several new components to decarbonize the steel syngas. In order to minimize the efficiency penalty while reduc-ing the number of new reactors adopted, different plant solutions can be designed. Here, two different plant layouts are proposed and discussed. In both cases the energy penalty to capture CO_2 is determined by the steam requirements for the shift reaction and the SEWGS rinse and purge. As shown in (Manzolini et al., 2011), the plant performance is maximized when a tight heat integration between the heat recovery steam cycle and the SEWGS process is considered. Accordingly, steam requirements are satisfied by bleeding from the turbine or the HRSG.

3.4.1. *SEWGS with steam/CO_2 expander (SEWGS EXP)*

Fig. 6 shows the first SEWGS plant. After the compression and the steam mixing, the steel mill off-gas enters a conventional HTS reactor, where the largest part of CO is converted into H_2; two compressor intercoolers are adopted in order to match the compressed fuel temperature with the typical HTS inlet temperatures (300–350 °C). The shifted gas is produced at about 450 °C and is cooled to 400 °C producing HP steam before entering the SEWGS unit. Two different streams, both at high temperature (430 °C), leave the SEWGS: (i) the hydrogen rich flow, which is sent to the GT and (ii) the $CO_2 + H_2O$ flow. The GT fuel is cooled to 350 °C, assumed as the maximum temperature of GT fuel injection, by producing HP steam before entering the combustor. Thanks to the high steam content, the H_2O/CO_2 rich gas can be expanded in a turbine as proposed in (Gazzani et al., 2013a) thus increasing the efficiency of the heat energy recovery. Although the optimal outlet pressure is function of the amount of steam used for the SEWGS regener-ation and should change accordingly for every SEWGS operating conditions, it has been fixed to 0.5 bar throughout all cases as this is the minimum pressure that allows deriving the SEWGS steam from the power island. After the expansion and further cooling

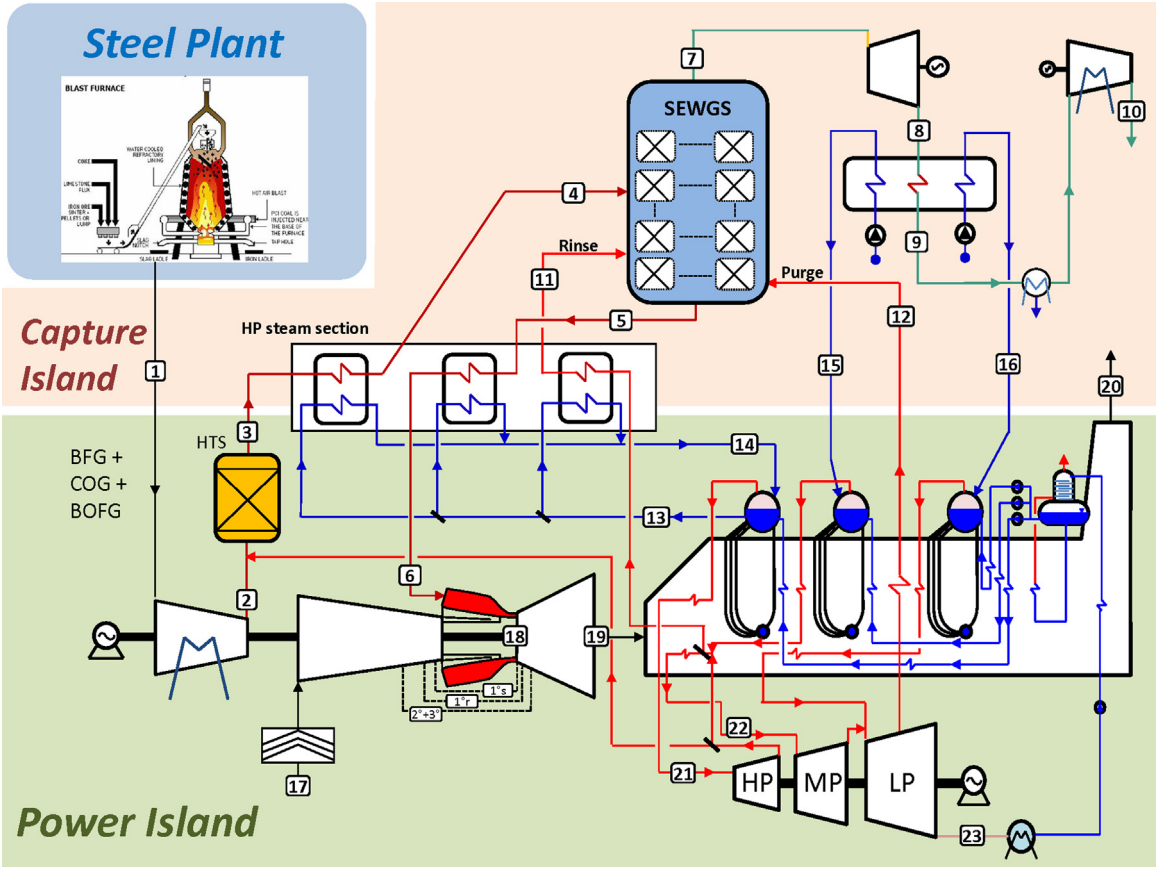

Fig. 6. Plant layout for pre-combustion CO_2 capture in an integrated steelworks using the SEWGS process with steam/CO_2 expander.

Table 6
Mass flow, temperature, pressure and composition for SEWGS with steam/CO_2 expander. Numbers refer to Fig.6.

Stream	$\dot{m}$ (kg/s)	T (°C)	p (bar)	Composition (%mol.)							
				$CH_4 + C_2H_4$	CO	CO_2	H_2	H_2O	Ar	N_2	O_2
1	180.0	30.0	1.01	Steel plant gas as reported in Table 1							
2	180.0	325.0	28.30								
3	225.2	448.5	27.60	1.69	3.60	25.50	16.67	17.28	–	35.27	–
4	225.2	400.0	27.54	1.69	3.60	25.50	16.67	17.28	–	35.27	–
5	109.0	427.0	27.26	2.53	0.17	0.70	29.86	14.48	–	52.26	–
6	109.0	350.0	27.26	2.53	0.17	0.70	29.86	14.48	–	52.26	–
7	143.7	426.8	1.05	–	0.01	56.56	0.23	42.78	–	0.42	–
8	143.7	350.2	0.50	–	0.01	56.56	0.23	42.78	–	0.42	–
9	143.7	35.0	0.50	–	0.01	56.56	0.23	42.78	–	0.42	–
10	115.6	35.0	110.00	–	0.01	98.85	0.41	–	–	0.73	–
11	13.4	400.0	28.00	–	–	–	–	100	–	–	–
12	14.0	400.0	1.25	–	–	–	–	100	–	–	–
13	28.6	330.8	130.00	–	–	–	–	100	–	–	–
14	28.6	335.0	130.00	–	–	–	–	100	–	–	–
15	11.7	231.3	28.10	–	–	–	–	100	–	–	–
16	14.0	186.9	1.26	–	–	–	–	100	–	–	–
17	394.0	15.0	1.01	–	–	0.04	–	1.03	0.92	77.28	20.73
18	386.0	1458.0	17.61	–	–	1.50	–	20.50	0.61	71.90	5.49
19	503.0	598.5	1.04	–	–	1.18	–	16.26	0.68	73.07	8.81
20	503.0	103.7	1.01	–	–	1.18	–	16.26	0.68	73.07	8.81
21	79.0	559.5	120.90	–	–	–	–	100	–	–	–
22	37.7	561.0	22.96	–	–	–	–	100	–	–	–
23	33.8	32.2	0.048	–	–	–	–	100	–	–	–
Net power output: 229.5 MW				**Net electric efficiency: 37.65%**						**CO_2 emissions: 149 g/kWh$_{el}$**	

steps, the water is condensed and the CO_2 is compressed for final transport and storage. Heat and mass balances of the SEWGS EXP plant are reported in Table 6. The resulting net power output is 229.5 MW with a net electric efficiency of 37.7% and CO_2 emissions of 149 g/kWh$_{el}$, which corresponds to CO_2 avoided of about 89%.

3.4.2. *SEWGS with syngas saturator (SEWGS SAT)*

Fig. 7 shows the second SEWGS plant layout. In this configuration, the compressed steel mill off-gas is sent to a saturator in order to reduce the steam consumption for the HTS reaction. The saturator water is heated by recovering heat from the inter-cooled compressor and from the hot CO_2 stream exiting the SEWGS.

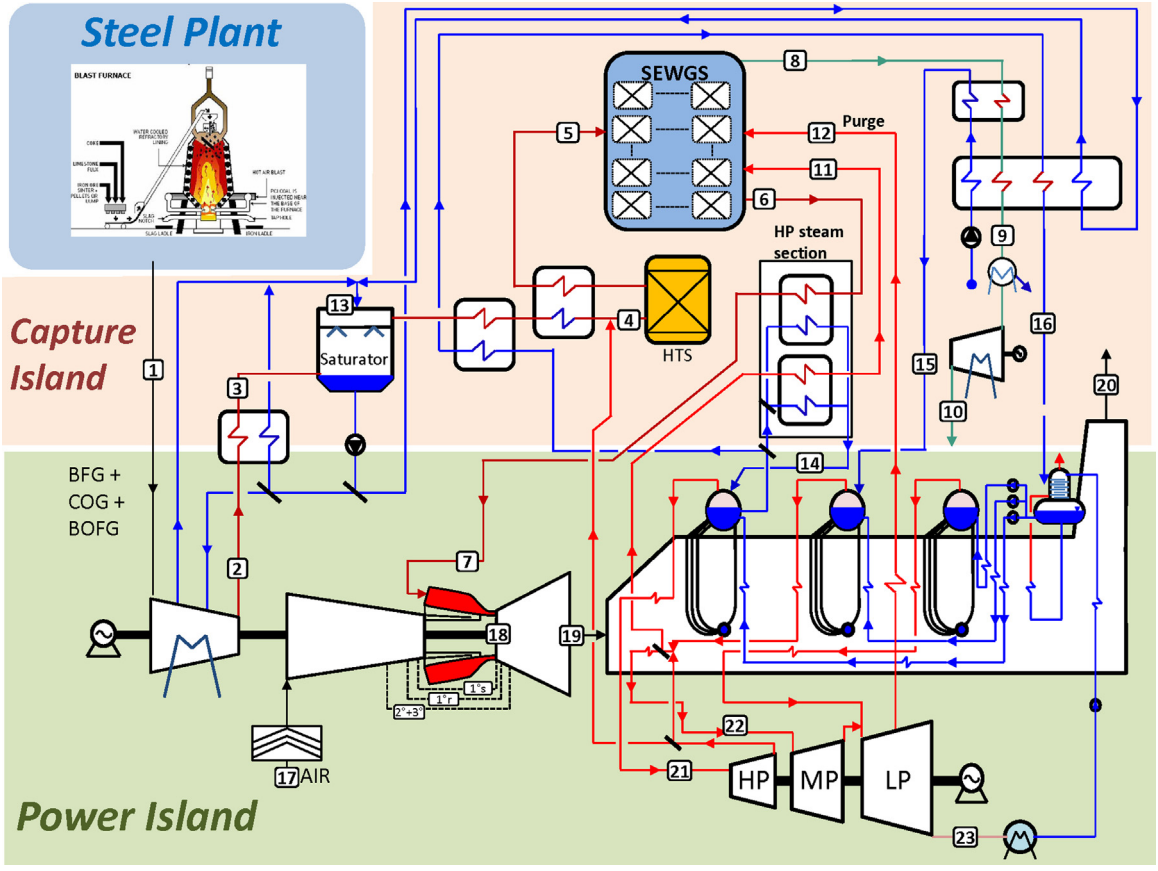

Fig. 7. Plant layout for pre-combustion CO_2 capture in an integrated steelworks using the SEWGS process with saturator.

Table 7
Mass flow, temperature, pressure and composition for SEWGS with saturator. Streams numbers refer to Fig.7.

Stream	$\dot{m}$ (kg/s)	T (°C)	p (bar)	Composition (%mol.)							
				$CH_4 + C_2H_4$	CO	CO_2	H_2	H_2O	Ar	N_2	O_2
1	180.0	30.0	1.01	Steel Plant gas as reported in Table 1							
2	180.0	220.3	28.30								
3	180.0	102.6	28.30								
4	225.2	320.0	28.02	1.69	15.16	13.94	5.14	28.80	–	35.27	–
5	225.2	400.0	28.02	1.69	3.60	25.50	16.67	17.28	–	35.27	–
6	109.0	427.0	27.18	2.53	0.17	0.70	29.86	14.48	–	52.25	–
7	109.0	350.0	27.18	2.53	0.17	0.70	29.86	14.48	–	52.25	–
8	143.7	426.7	1.05	–	0.01	56.56	0.23	42.78	–	0.42	–
9	143.7	78.6	1.05	–	0.01	56.56	0.23	42.78	–	0.42	–
10	112.4	35.0	1.05	–	0.01	98.85	0.41	–	–	0.73	–
11	13.4	400.0	28.00	–	–	–	–	100	–	–	–
12	14.0	400.0	1.25	–	–	–	–	100	–	–	–
13	139.1	210.3	28.30	–	–	–	–	100	–	–	–
14	16.0	335.0	130.00	–	–	–	–	100	–	–	–
15	17.6	231.3	28.10	–	–	–	–	100	–	–	–
16	32.4	330.8	130.00	–	–	–	–	100	–	–	–
17	393.9	15.0	1.01	–	–	0.04	–	1.03	0.92	77.28	20.73
18	385.9	1458.2	17.61	–	–	1.50	–	20.50	0.61	71.90	5.49
19	502.9	598.5	1.04	–	–	1.18	–	16.26	0.68	73.07	8.81
20	502.9	102.2	1.01	–	–	1.18	–	16.26	0.68	73.07	8.81
21	62.5	559.5	120.90	–	–	–	–	100	–	–	–
22	46.8	561.0	22.96	–	–	–	–	100	–	–	–
23	42.5	32.2	0.048	–	–	–	–	100	–	–	–
Net power output: 229.7 MW				**Net electric efficiency: 37.69%**						**CO_2 emissions: 149 g/kWh$_{el}$**	

Steel mill off-gas compression features three intercooled stages (vs. two of the previous configuration). This is made in order to reduce electric consumption for gas compression and considering that compressor outlet temperature does not have to match the HT-WGS inlet temperature, but be suitable for saturator operation. The saturated syngas is heated up to 320 °C before entering the HTS through a regenerative heat exchanger. As in the first SEWGS con-figuration, the hydrogen rich stream enters the GT combustor at 350 °C, whilst the CO_2 + H_2O stream is cooled producing MP steam and heating additional process water. Given that the heat recovery management is largely affected by the need of heat for the saturator, the SEWGS CO_2 + H_2O stream is not expanded as in *SEWGS EXP* configuration. The available heat is instead entirely used to produce medium and low pressure steam as well as to heat up the saturator water. Heat and mass balances of the SEWGS SAT plant are reported in Table 7. The resulting net power output is 229.7 MW with a net electric efficiency of 37.7% and CO_2 emissions of 148.9 g/kWh$_{el}$, which corresponds to CO_2 avoided of about 89%.

4. Results and discussion

Table 8 summarizes the thermodynamic performance of all the proposed plant layouts. REF$_{withNG}$ case has a net electric efficiency of 54.9% and specific emissions of about 851 g_{CO_2}/kWh$_{el}$. The efficiency is lower than a state-of-the-art NGCC plant because of the steel mill syngas compression (34 MW$_{el}$, corresponding to an efficiency penalty of 5.8 percentage points) while the high specific CO_2 emissions are due to the large carbon content in the fuel. REF$_{w/oNG}$ case features a decrease in the performance (the net electric efficiency is 52.3%) because NG is not used and the power to compress the steel mill syngas flow increases accordingly (67 MW$_{el}$). Apart from this, due to the assumed constant gas cycle parameters, the gas turbine and the steam cycle power productions are not sig-nificantly affected by the change of fuel. It is worthwhile noting the specific emission increase to about 1340 g_{CO_2}/kWh$_{el}$, which is almost twice the emission of a modern coal based power plant.

The performance of the cases with MEA post-combustion capture is reported in the third and fourth columns of Table 8 for MEA$_{withNG}$ and MEA$_{w/oNG}$, respectively. Either using natural gas or pure steel mill syngas, the CO_2 capture ratio is largely affected by the steam consumption for the solvent regeneration. Looking at MEA$_{withNG}$, the gas turbine power output is unaffected compared to the reference case (REF$_{withNG}$) whilst the steam power output drops from 116 MW to about 62 MW. Summing this loss with the CO_2 capture and compression consumptions, the net electric efficiency decreases to 41.5% with about 13.5 percentage points
decay. Despite the efficiency penalization, the CO_2 avoided does not reach the typical 85–90% of an amine plant but is limited to 66%. The remarkable power decrease along with the limited CO_2 capture brings about a rather high SPECCA, 3.8 MJ/kg_{CO_2}. A similar decrease of the net electric efficiency (13.6 percentage points) can be noticed by comparing the MEA case without natural gas addition (MEA$_{w/oNG}$) with its respective reference case (REF$_{w/oNG}$). On the other hand, given that the amount of steam generated is similar in the two MEA cases but the specific CO_2 emission of the reference without natural gas is significantly higher (1338 g_{CO_2}/kWh), the CO_2 avoided drops to 35%, with a resulting SPECCA of 5.2 MJ/kg_{CO_2}. From these results, the application of a conventional amine scrubbing process for CO_2 capture from a combined cycle coupled with an integrated steel plant does not represent an attractive solution, independently of the blending with natural gas.

Concerning the pre-combustion capture route, the MDEA process allows capturing about 90% of the CO_2 with a commercially available technology. Compared to the MEA$_{w/oNG}$ case with capture, a higher steam turbine power output is obtained in spite of the higher carbon capture ratio, thanks to the lower heat demand for solvent regeneration. On the other hand, higher consumptions are obtained for CO_2 compression, due to the higher capture efficiency, and for fuel compression (75.5 MW), resulting in a lower power output at the GT shaft. This leads to a lower net power output and electric efficiency. The resulting SPECCA of 2.9 MJ/kg_{CO_2} is however significantly lower than the post-combustion capture cases as consequence of the higher CO_2 capture rate.

Finally, in the last four columns of the table, the SEWGS cases are presented divided according to the plant configuration (EXP or SAT) and to the sorbent adopted (α or β, case 3 and 11 of Table 5, respectively). Similarly to the MDEA case, the steel mill syngas compression accounts for a larger power penalization than in the reference and MEA cases. An intermediate power output at the GT shaft is obtained in this case, due to the additional contribution to the GT

Table 8
Power balances for the different combined cycle integrated with the steel plant, from the left: reference no capture, MEA-based capture, MDEA-based capture, SEWGS-based capture with steam/CO_2 expander and SEWGS-based capture with saturator.

	REF with NG	REF w/o NG	MEA with NG	MEA w/o NG	MDEA	SEWGS EXP		SEWGS SAT	
Steel plant off-gas input, kg/s	90.0	180.0	90.0	180.0	180.0	180.0	180.0	180.0	180.0
Steel plant off-gas input, MW_{LHV}	304.9	609.8	304.9	609.8	609.5	609.5	609.5	609.5	609.5
Steel plant off-gas compression, MW_{mech}	33.5	66.5	33.5	66.5	75.5	77.3	77.3	75.5	75.5
NG input, kg/s	5.9	–	5.9	–	–	–	–	–	–
NG input, MW_{LHV}	271.9	–	271.9	–	–	–	–	–	–
LHV mixture, kJ/Nm^3	7509.7	4386.1	7509.7	4386.1	4383.5	4383.5	4383.5	4383.5	4383.5
Total heat input, MW_{LHV}	576.8	609.8	576.8	609.8	609.5	609.5	609.5	609.5	609.5
Sorbent type	–	–	–	–	–	α	β	α	β
Power production									
Gas turbine*, MW_{el}	204.1	199.0	204.1	199.0	181.1	190.7	188.3	192.1	190.1
Steam turbine, MW_{el}	116.0	123.32	62.4	66.6	76.6	61.2	75.8	62.6	80.4
CO_2/H_2O SEWGS expander, MW_{el}	–	–	–	–	–	17.6	14.2	0.0	0.0
Consumptions									
Steam cycle pumps, MW_{el}	1.5	1.5	1.5	1.5	1.4	1.7	1.7	2.1	2.0
CO_2 compression, MW_{el}	–	–	17.5	19.5	36.7	42.2	45.8	36.0	37.2
MEA/MDEA auxiliaries, MW_{el}	–	–	7.9	8.5	7.6	–	–	–	–
Steam cycle heat rejection, MW_{el}	1.5	1.64	–	–	0.5	1.3	1.3	1.5	1.4
Balance of plant, MW_{el}	0.2	0.4	0.2	0.4	0.4	0.1	0.1	0.2	0.2
Balance									
Net power output, MW_{el}	316.9	318.8	239.5	235.7	211.1	224.2	229.5	215.0	229.7
Net electric efficiency, $\%_{LHV}$	**54.95**	**52.28**	**41.53**	**38.65**	**34.64**	**36.78**	**37.65**	**35.27**	**37.69**
CO_2 specific emissions, g/kWh_{el}	850.6	1339.5	291.6	871.0	147.1	291.0	149.1	215.6	148.9
Avoided CO_2, %	–	–	65.7	35.0	89.3	78.3	88.9	83.9	88.9
SPECCA, MJ_{LHV}/kg_{CO_2}	–	–	**3.79**	**5.20**	**2.94**	**2.77**	**2.25**	**2.95**	**2.24**

* Includes the steel mill off-gas compression power.

power generation from the expansion of the steam in the fuel mixture. As a matter of fact, the H_2-based fuel produced by the SEWGS process is highly diluted with the excess steam used for the WGS reaction. In all the SEWGS cases, a similar GT output is obtained. The main differences in the net power output and efficiency are due to: (i) the steam turbine power output, (ii) the adoption of the post-SEWGS expander, and (iii) the CO_2 compressor inlet pressure. The steam cycle power output depends on the sorbent type and the CO_2 capture ratio set in the SEWGS—the higher the capture, the higher the steam consumption for the bed regeneration. Cases with sorbent α require more steam and hence show a lower steam turbine power output (see Table 8) even with lower CO_2 capture ratio. The adoption of the expander downstream the SEWGS increases the gross power generation thanks to the significant power output resulting from the steam/CO_2 rich stream expansion. The additional power output is however somewhat balanced by the increased consumption for CO_2 compression. The CO_2 avoided ranges between 78% and 89%—with sorbent α and β respectively. The resulting SPECCA is between 3 and 2.24 MJ/kg_{CO_2}. Accordingly, SEWGS per-forms better than the MEA post-combustion for any given operating conditions/sorbent, whilst sorbent β must be adopted to outper-form the MDEA pre-combustion capture case.

4.1. Strategies to improve the post-combustion MEA-based plants

Results have shown that the conventional MEA process does not allow reaching high carbon capture and that the resulting efficiency penalization is rather high. On the other hand, the amine-based scrubbing is the most mature technology for carbon capture due to the number of demonstration plants running and technology licensors offering a commercial process. Therefore, it is important to improve the competitiveness of this process and keep it as valid alternative for CO_2 capture in an integrated steelworks. Accordingly, new plant solutions that aim at improving the CO_2 capture level and/or simplifying the capture section were assessed. Fig. 8 and Table 9 show the plant configurations proposed and the thermodynamic results, respectively. Only MEA with addition of natural gas has been considered for this analysis due to the very poor capture performance of $MEA_{w/oNG}$.

(a) **Flue gas by-pass at the HRSG stack**: This solution simplifies the capture section by decreasing the flue gas flow treated in the amine plant while allowing the MEA plant to work closer to conventional design conditions. In order to achieve 90% carbon capture of the flue gas entering the absorber, around 15% of the total flue gas is vented before the capture section. Compared to the conventional MEA, this solution features (i) a smaller column diameter—thus with benefits on the CAPEX, (ii) lower consumption of the flue gas fan and (iii) lower heat rejection consumption for flue gas cooling. On the other side, the CO_2 avoided slightly decreases, while the SPECCA does not significantly change.

(b) **Auxiliary boiler**: The main limit of the conventional MEA is determined by the lack of steam for the solvent regeneration needed to capture 90% of the entering CO_2. With this solution part of the steel mill off-gas is burned in an auxiliary boiler producing the additional low pressure steam to achieve the 90% CO_2 capture. The boiler flue gases are mixed with the GT gases and treated in the MEA plant. The gas turbine net power output is kept constant by increasing the natural gas heat input. The CO_2 avoided increases to about 86% while the efficiency decreases to 37.7% due to the higher thermal power input used for LP steam generation only. The resulting SPECCA is 4.1 MJ/kg_{CO_2}. The production of high pressure steam in the auxiliary boiler, which can be expanded in the steam turbine, can be considered as an advanced version of this configuration. In this case the performance would increase at the expenses of the plant complexity and cost.

(c) **Post-fired combined cycle**: This solution aims at increasing the steam production in the plant along the same line of the previous configuration. This can be efficiently done by burning part of the steel mill syngas in a conventional post-firing burner at the HRSG inlet rather than in a dedicated boiler. The resulting plant performance benefits of a larger steam production and a

Table 9
Power balances of the different solutions proposed to increase the CO_2 capture in a steel plant with MEA-based post-combustion process.

	MEA flue gas by-pass	MEA auxiliary boiler	MEA post-firing	MEA + +NG
Steel mill off-gas input to GT combustor, kg/s	90.0	73.8	59.2	90.0
Steel mill off-gas input to GT combustor, MW_{LHV}	304.9	250.0	200.7	304.9
Other steel mill off-gas input, kg/s	–	16.2	30.8	–
Other steel mill off-gas input, MW_{LHV}	–	54.9	104.2	–
Steel plant off-gas compression, MW_{mech}	33.5	27.6	22.3	33.5
NG input, kg/s	5.9	7.0	8.1	10.8
NG input, MW_{LHV}	271.9	326.8	376.5	502.0
LHV mixture, kJ/Nm^3	7509.7	8311.0	10333.5	9724.3
Total Power input, MW_{LHV}	576.8	631.7	681.4	806.9
POWER PRODUCTION				
Gas turbine, MW_{el}	204.1	207.4	210.4	292.7
Steam turbine, MW_{el}	62.4	62.3	93.4	87.9
CO_2/H_2O SEWGS expander, MW_{el}	–	–	–	–
CONSUMPTIONS				
Steam cycle pumps, MW_{el}	1.5	1.5	2.2	2.0
CO_2 compressor, MW_{el}	17.5	21.3	22.9	24.5
MEA/MDEA auxiliaries, MW_{el}	7.4	8.9	9.0	11.8
Steam cycle heat rejection, MW_{el}	–	–	–	–
Balance of Plant, MW_{el}	0.2	0.1	0.1	0.2
BALANCE				
Net power output, MW_{el}	240.1	237.9	269.6	342.1
Net electric efficiency, $\%_{LHV}$	**41.62**	**37.65**	**39.56**	**42.39**
CO_2 specific emissions, g/kWh_{el}	293.0	116.5	125.2	109.3
Avoided CO_2, %	65.6	86.3	85.3	87.2
SPECCA, MJ_{LHV}/kg_{CO_2}	**3.76**	**4.10**	**3.51**	**2.62**

lower syngas compression duty (the post-firing fuel is burned at ambient pressure). The gas turbine size is kept constant by increasing natural gas heat input. In order to limit the plant cost, the HRSG is supposed to operate with simple duct burners that do not require the combustion chamber cooling. Accordingly, the gas temperature has been limited to 750 °C. The resulting CO_2 avoided increases to about 85% while the efficiency is 39.6%, thus with a contained decrease. The SPECCA is 3.5 MJ/kg_{CO_2}, lower than the reference MEA case discussed above.

(d) **Increased GT size**: The last plant layout makes use of a larger gas turbine where the additional heat input is supplied by natural gas. With this configuration the plant is more similar to a conventional combined cycle with increased availability of heat in the HRSG and lower CO_2 concentration in the combustion gas. Accordingly, the performance increases: the CO_2 avoided is 87% while the efficiency rises to 42.4%. The resulting SPECCA is 2.6 MJ/kg_{CO_2}.

4.2. SEWGS operating parameters

Considering the SEWGS process, several operating conditions (see Table 5) have been investigated for the two plant layouts developed. The resulting net electric efficiencies at different CO_2 capture levels in the SEWGS unit are summarized in Fig. 9. Firstly, two main areas can be identified depending on the sorbent adopted. When sorbent α is used, the maximum net electric efficiency achievable is 37% – for a SEWGS CCR of 90% – while it decreases to about 35%for 95% SEWGS CCR (i.e. higher CCR would require too much steam, exceeding the internal plant production). No significant differences in the efficiency arise between SEWGS SAT and SEWGS EXP. On the other hand it is worthwhile noting that the SEWGS EXP configu-ration cannot capture more than 90% CO_2, due to its lower steam production from H_2O/CO_2 cooling.

The adoption of sorbent β brings about a remarkable improve-ment in the net electric efficiency, with a minimum increase of two percentage points compared to sorbent α, as well as in the CO_2 capture level, which can reach 98%. For CCR equal to 90 and 95%, the SEWGS SAT features a higher efficiency compared to SEWGS EXP. At CCR 98% the high water content in the CO_2 stream produced by the SEWGS is exploited in the expander thus flattening the efficiency difference between the two plant configurations.

Referring to SEWGS SAT *sorbent β* with 95% CCR, Fig. 10 shows the sensitivity analysis on the main PSA-system sizing and operating variables i.e.: column length, number of vessels and cycle time. In the larger image, *S/C* (thin bars) and resulting net electric efficiency (thick bars) are reported. In the smaller images on right hand side of Fig. 10, the effect of the reactor system variables on purge and rinse steam consumption is shown. It is worth noting that the purge steam varies steeply with the operating variables whilst the change in the rinse requirement is limited. It must be outlined that the exergy content of the two streams is significantly different: the purge steam is at ambient pressure while rinse is at high pres-sure. The second and third bars in Fig. 10 are representative of this difference: the two cases have very similar efficiency even with totally different rinse and sweep flowrates. The sharp decrease of the purge, achieved by increasing the column length, is counterbal-anced by a limited increase in the rinse steam. Therefore, a small change in the rinse steam can significantly affect the steam cycle power output. Similarly, decreasing the vessel number (2nd vs 4th bar in Fig. 10) requires a larger purge flow to keep the same CO_2 capture but also lowers the rinse flow, which is proportional to the total SEWGS volume; the resulting efficiency is almost unaffected. The optimal SEWGS design should be established through a detailed techno-economic analysis.

4.3. Effects of blending the steel mill off-gas with natural gas

In the analysis presented above, the performance of the capture cases has been compared to their respective plants without CO_2 capture by considering the same type of fuel input, i.e.: the REF_{withNG} or the $REF_{w/oNG}$ cases have been used as reference plants for the MEA_{withNG} and $MEA_{w/oNG}$ cases respectively, while in all the other cases the $REF_{w/oNG}$ plant has been considered as reference. Though this permits to fairly evaluate the capture performance of each technology, it makes the comparison between cases with and without natural gas blending and among cases with NG blending but different NG thermal inputs difficult. Given that the present work focuses on the CO_2 capture from the integrated steel mill fuel gas, we aim at defining performance indexes referred to steel

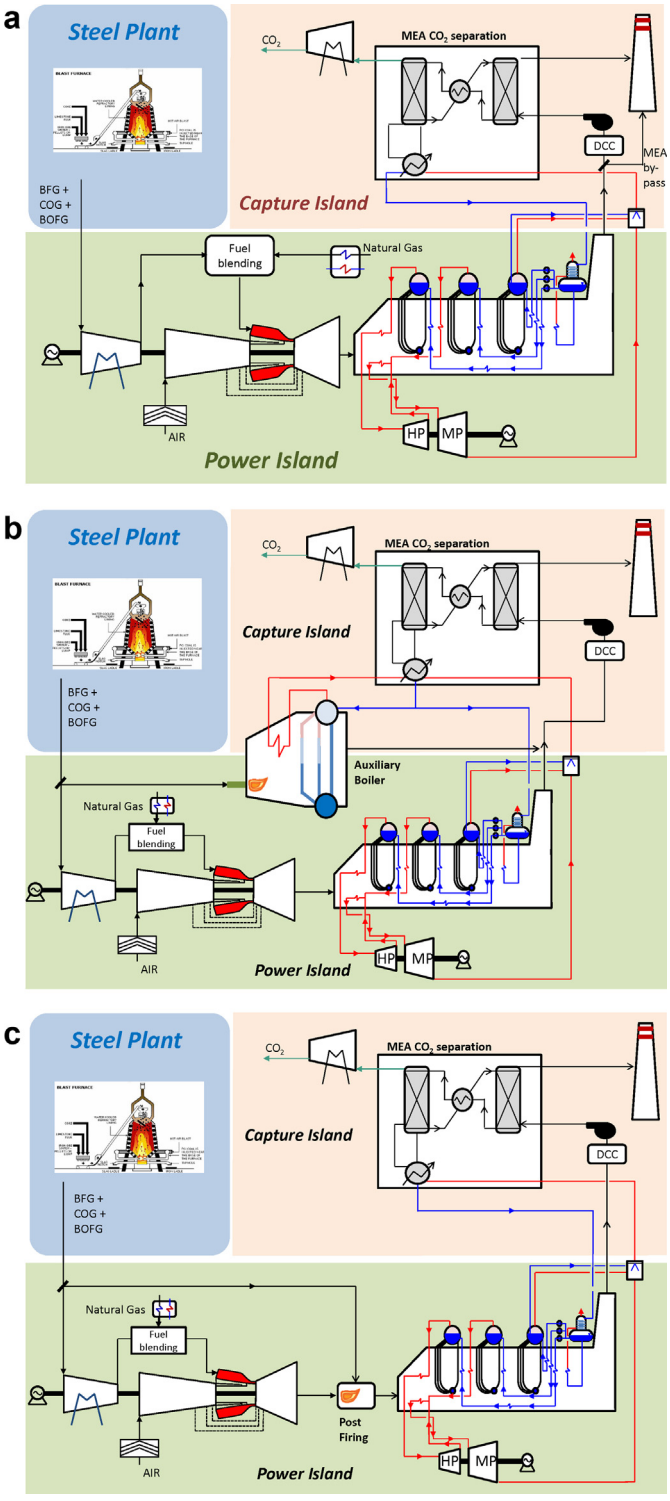

Fig. 8. Layout of the different alternatives for enhanced CO_2 capture with MEA. (a) use of by-pass before the MEA section, (b) use of an auxiliary boiler to provide extra steam to the MEA process and, (c) use of post-firing to increase the steam production of the HRSG.

mill off-gas utilization also for the plants with natural gas blending. This is accomplished by considering the performance of reference natural gas to electricity plants, namely a natural gas combined cycle (NGCC) without capture with an efficiency $\eta_{NG\ ref}$ of 58.3% and specific emissions $e_{NG\ ref}$ of 352 g/kWh, and a NGCC with post-combustion MEA capture with an efficiency $\eta_{NG\ ref}$ of 49.9% and specific emissions $e_{NG\ ref}$ of 41 g/kWh (Franco et al., 2011;

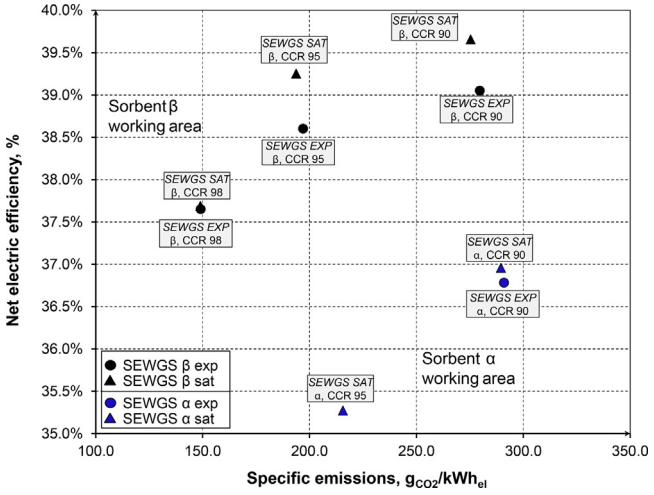

Fig. 9. Net electric efficiency and specific emissions for different SEWGS solutions (i.e., sorbent type and plant layout). Triangles refer to the SEWGS plant with saturator while circles refer to the SEWGS plant with steam/CO_2 expander.

Manzolini et al., 2011). Once the power output and CO_2 emissions referred to the natural gas have been calculated through Eqs. (4)–(5), the equivalent power output, efficiency and emissions associated to the steel mill off-gas conversion can be determined through Eqs. (6)–(9).

$$P_{NG} = \dot{m}_{NG} LHV_{NG} \eta_{NG\_ref} \tag{4}$$

$$E_{NG} = P_{NG} e_{NG\_ref} \tag{5}$$

$$P_{steel\ gas} = P_{tot} - P_{NG} \tag{6}$$

$$\eta_{steel\ gas} = \frac{P_{steel\ gas}}{\dot{m}_{steel\ gas} LHV_{steel\ gas}} \tag{7}$$

$$E_{steel\ gas} = E_{tot} - E_{NG} \tag{8}$$

$$e_{steel\ gas} = \frac{E_{steel\ gas}}{P_{steel\ gas}} \tag{9}$$

Results are shown in Fig. 11 and Table 10. In Fig. 11, two efficiency and SPECCA bars are reported, which differ when natural gas is used in the plant: (i) on the left hand side, in blue, the overall efficiency of the plant with the mixed fuel (already reported in the previous tables) and (ii) on the right hand side, in grey, the efficiency corresponding to the conversion of the steel mill syngas only $\eta_{steel\ gas}$. Similarly, thin bars overlaying the efficiency are used to compare the two SPECCAs: on the left, the overall SPECCA corresponding to the use of mixed fuel and, on the right, the SPECCA ascribable to the steel mill syngas use exclusively (i.e., calculated using $\eta_{steel\ gas}$ and $E_{steel\ gas}$ as performance indexes and considering the $REF_{w/oNG}$ case as reference).

First, it can be observed that the equivalent efficiency of the case REF_{withNG} (51.9%) gets close to the $REF_{w/oNG}$ case one (52.3%). The same is true for the equivalent specific emissions (1348 vs. 1339 g/kWh). This indicates that the conversion of natural gas by blending steel gas in a combined cycle is obtained with a similar efficiency of a stand-alone NG-fired combined cycle. In other words, the efficiency and specific emissions of a NG-steel gas combined cycle can be obtained with a good accuracy as a weighted average of the performance of an unblended NG-fired and a steel mill syngas-fired combined cycles.

With reference to the MEA_{withNG} case, a significant efficiency decrease to below 35% is obtained when natural gas contribution is excluded. Such equivalent efficiency is lower than the efficiency of the unblended $MEA_{w/oNG}$ case. This is due to the additional

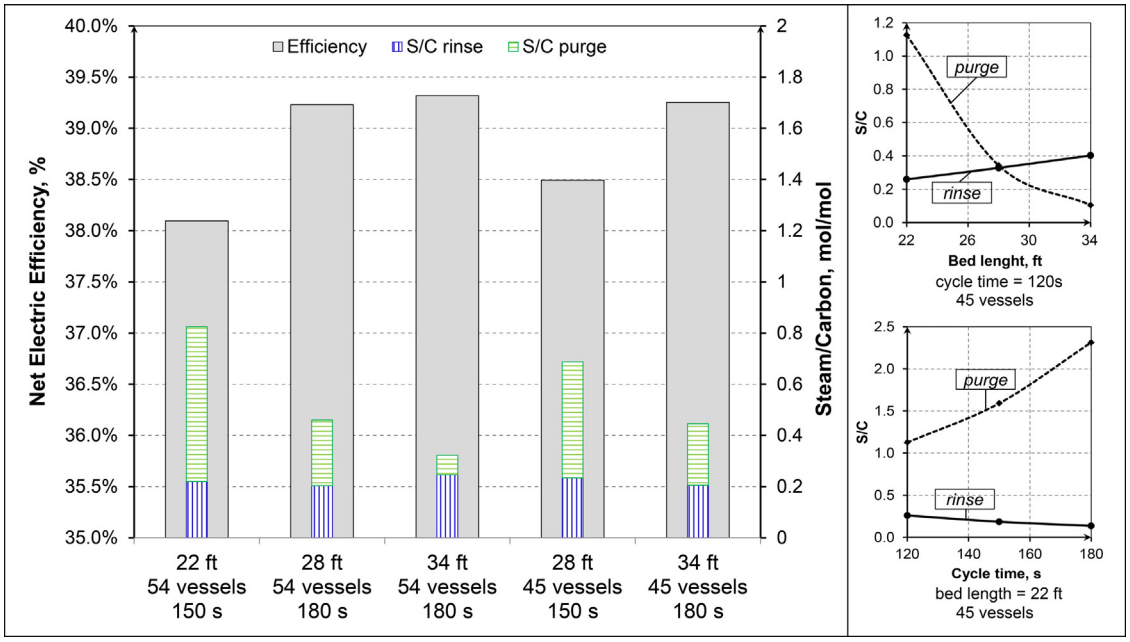

Fig. 10. Net electric efficiency and required steam-to-carbon ratio for different SEWGS operating conditions (vessel length, number and cycle time). Numbers refer to the SEWGS SAT configuration using sorbent type β, with 95% CCR. The lower inner bar (blue) refers to the rinse *S*/*C* whilst the upper inner bar (green) refers to the purge *S*/*C*. On the right hand side, the purge and rinse *S*/*C* variation with the bed length and cycle time is shown. (For interpretation of the references to color, the reader is referred to the web version of this article).

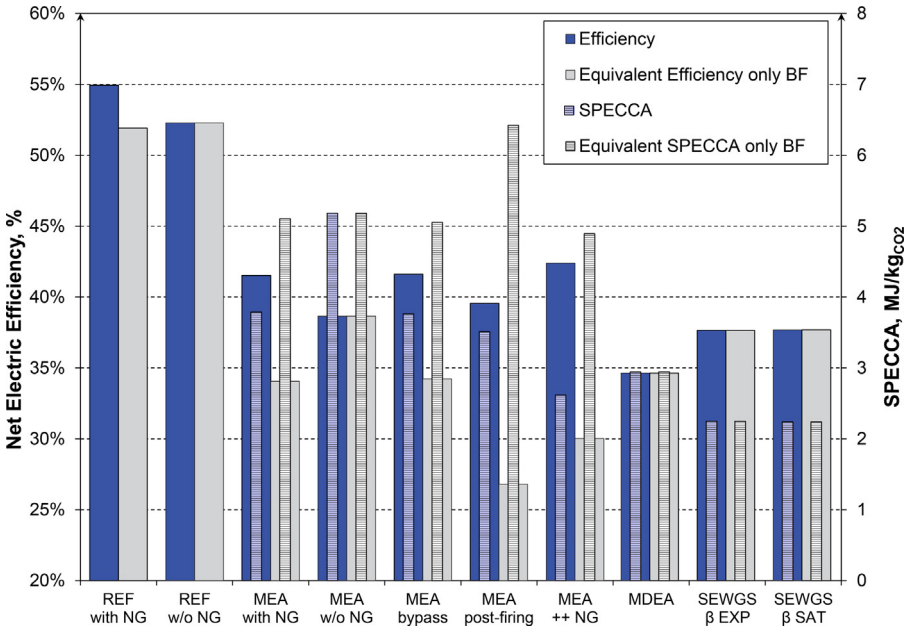

Fig. 11. Repartition of the net electric efficiency and SPECCA between the natural gas and the steel mill syngas. For each case: The bars on the left, either for the efficiency or the SPECCA, refer to the performance with the mixed fuel whilst the bars on the right refer to the use of steel syngas only. (For interpretation of the references to color, the reader is referred to the web version of this article).

efficiency penalty caused by the higher CO_2 capture efficiency consequence of the supplementary heat from natural gas blending. As a matter of fact, the resulting equivalent emissions of 619 g/kWh of the MEA_{withNG} case (Table 10) is significantly lower than 871 g/kWh

Table 10
Equivalent efficiency, CO_2 specific emissions and SPECCA of the reference and MEA cases with steel mill gas-NG blending.

	REF with NG	MEA with NG	MEA bypass	MEA Post-firing	MEA++NG
Equivalent efficiency, %	51.92	34.06	34.23	26.79	42.39
Equivalent specific emissions, g_{CO_2}/kWh_{el}	1348	619	620	318	296
Equivalent SPECCA, MJ/kg_{CO_2}	–	5.11	5.05	6.42	4.89

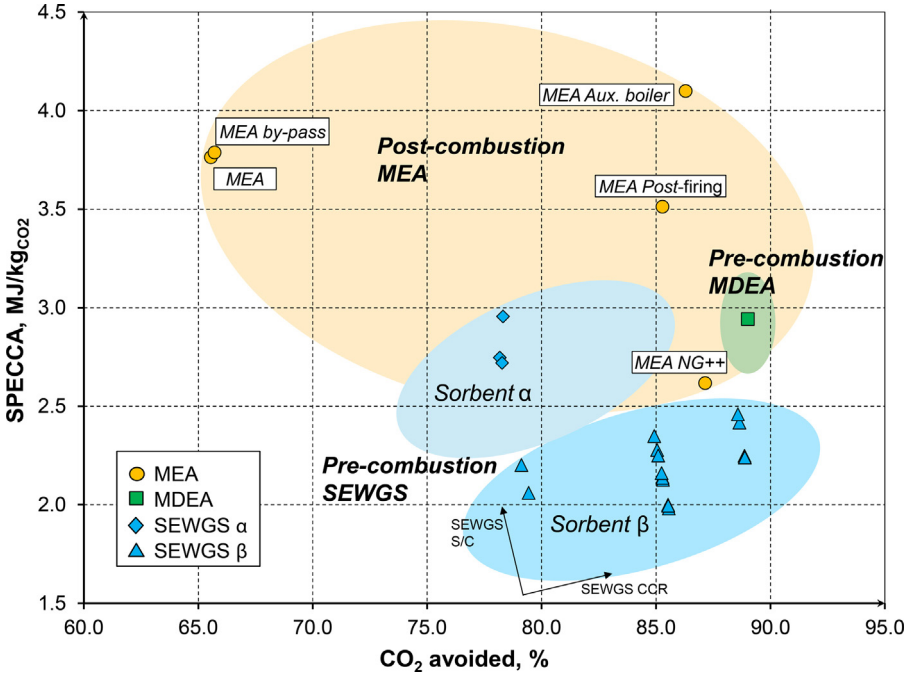

Fig. 12. Comparison of the different plant solutions proposed in term of CO_2 avoided and SPECCA. Macro areas for each technology can be drawn: MEA features high SPECCA and wide variation in the CO_2 avoided; MDEA has almost 90% capture efficiency with moderately high SPECCA. Finally, sorbent β SEWGS allows good CO_2 capture efficiencies with the lowest SPECCA values. (For interpretation of the references to color, the reader is referred to the web version of this article).

of the $MEA_{w/oNG}$ case (Table 8). If the SPECCA of these two cases are compared, 5.0 vs. 5.2 MJ/kg_{CO_2} are obtained respectively for the two cases, showing a similar energy penalty for CO_2 avoided associated to the use of the steel mill off-gas. Similar considerations can be made for the MEA_{bypass} case (whose energy and material balances have minor differences with respect to the MEA_{withNG} case) and for the MEA_{++NG} one. For this last case, the equivalent efficiency and emissions further reduce to 30.0% and 296 g/kWh, but the SPECCA remains close to 5 MJ/kg (specifically 4.8 MJ/kg).

A different result is obtained for the MEA post-firing case, where a significant fraction (about one third) of the steel mill syngas energy is burned in the HRSG post-firing burners. The equivalent net electric efficiency drops to about 27%, with equivalent CO_2 specific emissions of 318 g/kWh. A resulting equivalent SPECCA of 6.3 MJ/kg_{CO_2} is obtained, much higher than the previous cases, as consequence of the lower conversion efficiency of the post-firing fuel. Even worse equivalent performance are obtained for the MEA with auxiliary boiler case, which is not reported in the figure.

If the equivalent performances of the MEA cases with fuel blending are compared to the MDEA and SEWGS cases, the better performance of the plants based on pre-combustion capture systems becomes evident in terms of higher efficiency (especially in the SEWGS cases) and much lower SPECCA.

5. Conclusions

Iron and steel industry is one of the most important contributors to anthropogenic CO_2 emissions accounting for about 5% of the total emissions. In this work, different CO_2 mitigation solutions in integrated steel plant were investigated.

Two commercially available CO_2 capture technologies based on post-combustion MEA and pre-combustion MDEA scrubbing as well as the innovative sorption enhanced water gas shift (SEWGS) process were considered and compared. For each technology, different plant configurations and operating conditions were evaluated. The overall results of this analysis are summarized in Fig. 12 where the capture level and the resulting SPECCA are shown for all the cases assessed in this work.

The adoption of conventional post-combustion MEA process permits to achieve 65% CO_2 avoidance with a SPECCA of about 3.8 MJ/kg_{CO_2}. Considering that the power plant normally accounts for 40–70% of the total emissions from an integrated steel mill, this corresponds to an overall CO_2 emissions reduction of about 25–45%. The capture level of the MEA process was improved by developing alternative plant configurations. CO_2 avoidance up to 85% (35–60% of the overall steel plant) was achieved with SPECCA values ranging between 4.1 and 2.7 MJ/kg_{CO_2}.

Considering the MDEA-based pre-combustion technology, the CO_2 capture level increases, reaching about 90% of CO_2 avoidance (35–65% of the overall steel plant) with a SPECCA of 3 MJ/kg_{CO_2}.

The adoption of the SEWGS technology allows both decreasing the primary energy consumption – SPECCA ranges between 2.0 MJ/kg_{CO_2} and 3.0 MJ/kg_{CO_2} – and increasing the CO_2 avoidance close to 90%. The SEWGS performance is affected by the plant configuration, the operating conditions and, most of all, the type of sorbent employed. The best configuration features the most advanced sorbent (Sorbent β) and the use of a saturator to limit the steam requirement for the shift.

From the results shown in Fig. 12, it can be noted that the pre-combustion plants perform better from a thermodynamic point of view. Moreover, differently from the power plant application, the syngas is already available from the steel plant, which is benefi-cial for the plant CAPEX (thus tackling the usual main drawback of pre-combustion configurations, where the syngas has to be produced through reforming or gasification). Nevertheless, the higher technology readiness level (TRL) and the number of existing and running plants make the MEA post-combustion solution an interesting alternative, for example in case of plant retrofitting.

Considering the continuous growth of steel production and the limited room for further improvement of the process energy efficiency, CO_2 capture in integrated steelworks seems an imperative solution. In this context, a mild capture process, which affects the power block exclusively, can play an important role for the existing

plants, where more advanced solutions cannot be deployed. Finally, the SEWGS process, which showed remarkable performance in capturing CO_2 from the overall steel mill off-gas, will be tested in a real steelworks plant as a direct blast furnace gas decarbonizing process. This test campaign, which is expected to bring the SEWGS process to TRL6, will be conducted under the Stepwise framework, a new European H2020 project.

Acknowledgments

The CAESAR project has received funding from the European Community's Seventh Framework Programme FP7/2007–2013 under grant agreement no. 213206.

References

Allam, R.J., Chiang, R., Hufton, J., Middleton, P., Weist, E.L., White, V., 2005. Development of the sorption enhanced water gas shift process. In: Carbon Dioxide Capture for Storage in Deep Geologic Formations. Elsevier Ltd, Oxford, UK.

Alstom Power, 2014. Alstom [WWW Document]. URL ⟨www.alstom.com/power⟩.

Arasto, A., Tsupari, E., Kärki, J., Pisilä, E., Sorsamäki, L., 2013. Post-combustion capture of CO_2 at an integrated steel mill—Part I: technical concept analysis. Int. J. Greenh. Gas Control 16, 271–277, http://dx.doi.org/10.1016/j.ijggc.2012.08.018

Birat, J., 2008. Steel and CO_2—the ULCOS Program, CCS and Mineral Carbonation using Steelmaking Slag. ArcelorMittal-Maizières-lès-Metz.

Boon, J., Cobden, P.D., van Dijk, H.a.J, Hoogland, C., van Selow, E.R., van Sint Annaland, M., 2014. Isotherm model for high-temperature, high-pressure adsorption of and on K-promoted hydrotalcite. Chem. Eng. J. 248, 406–414, http://dx.doi.org/10.1016/j.cej.2014.03.056

Boon, J., Cobden, P.D., van Dijk, H.a.J., van Sint Annaland, M., 2015. High-temperature pressure swing adsorption cycle design for sorption-enhanced water–gas shift. Chem. Eng. Sci. 122, 219–231, http://dx.doi.org/10.1016/j.ces.2014.09.034

Boyce, M.P., 2006. Gas Turbine Engineering Handbook, Third. ed. Gulf Professional Publishing, Burlington, MA, USA.

CACHET, 2008. CACHET FP6 project [WWW Document]. URL ⟨www.cachetco2.eu⟩.

CAESAR, 2010. CAESAR FP7 project [WWW Document].

Campanari, S., 2000. Full load and part-load performance prediction for integrated SOFC and microturbine systems. J. Eng. Gas Turbines Power 122, 239–246.

Campanari, S., Gazzani, M., Romano, M.C., 2012. Analysis of direct carbon fuel cell based coal fired power cycles with CO_2 capture. J. Eng. Gas Turbines Power 135, 011701, http://dx.doi.org/10.1115/1.4007354

Cheng, H.-H., Shen, J.-F., Tan, C.-S., 2010. CO_2 capture from hot stove gas in steel making process. Int. J. Greenh. Gas Control 4, 525–531, http://dx.doi.org/10.1016/j.ijggc.2009.12.006

Chiesa, P., Consonni, S., 2000. Natural gas fired combined cycles with low CO_2 emissions. J. Eng. Gas Turbines Power 122, 429.

Chiesa, P., Lozza, G., Mazzocchi, L., 2005. Using hydrogen as gas turbine fuel. J. Eng. Gas Turbines Power 127, 73, http://dx.doi.org/10.1115/1.1787513

Chiesa, P., Macchi, E., 2004. A thermodynamic analysis of different options to break 60% electric efficiency in combined cycle power plants. J. Eng. Gas Turbines Power 126, 770, http://dx.doi.org/10.1115/1.1771684

Consonni, S., 1992. Performance Prediction of Gas/Steam Cycles for Power Generation. Princeton University, Princeton, NJ, USA.

Dixon, T., Yamaji, K., Hayashi, M., Mimura, T., 2013. Steel industries in Japan achieve most efficient energy cut-off chemical absorption process for carbon dioxide capture from blast furnace gas. Energy Proc. 37, 7134–7138, http://dx.doi.org/10.1016/j.egypro.2013.06.650

Franco, F., Anantharaman, R., Bolland, O., Booth, N., van Dorst, E., Ekstrom, C., Sanchez Fernandes, E., Macchi, E., Manzolini, G., Nikolic, D., Pfeffer, A., Prins, M., Rezvani, S., Robinson, L., 2011. European best practice guidelines for assessment of CO_2 capture technologies.

Gazzani, M., Chiesa, P., Martelli, E., Sigali, S., Brunetti, I., 2014. Using hydrogen as gas turbine fuel: premixed versus diffusive flame combustors. J. Eng. Gas Turbines Power 136, 051504.

Gazzani, M., Macchi, E., Manzolini, G., 2013a. CO_2 capture in natural gas combined cycle with SEWGS. Part A: thermodynamic performances. Int. J. Greenh. Gas Control 12, 493–501.

Gazzani, M., Macchi, E., Manzolini, G., 2013b. CO_2 capture in integrated gasification combined cycle with SEWGS—Part A: thermodynamic performances. Fuel 105, 206–219.

Gazzani, M., Manzolini, G., MacChi, E., Ghoniem, A.F., 2013c. Reduced order modeling of the Shell-Prenflo entrained flow gasifier. Fuel 104, 822–837.

Gazzani, M., Romano, M., Manzolini, G., 2013d. Application of sorption enhanced water gas shift for carbon capture in integrated steelworks. Energy Procedia 37, 7125–7133, http://dx.doi.org/10.1016/j.egypro.2013.06.649

Goodman, N., 2007. Operations at the Hismelt Kwinana Plant, in: Proceedings of Iron & Steel Society International Technology Conference and Exhibition.

Helle, H., Helle, M., Saxén, H., Pettersson, F., 2010. Optimization of top gas recycling conditions under high oxygen enrichment in the blast furnace. ISIJ Int. 50, 931–938, http://dx.doi.org/10.2355/isijinternational.50.931

Ho, M.T., Bustamante, A., Wiley, D.E., 2013. Comparison of CO_2 capture economics for iron and steel mills. Int. J. Greenh. Gas Control 19, 145–159, http://dx.doi.org/10.1016/j.ijggc.2013.08.003

IEA, 2007. Tracking industrial energy efficiency and CO_2 emissions.

IEAGHG, 2013. Overview of the current state and development of CO_2 capture technologies in the ironmaking process.

IPCC, 2005. IPCC Special Report on Carbon Dioxide Capture and Storage. Cambridge University Press.

Jones, R., Goldmeer, J., Manager, P.M., Monetti, B., 2011. Addressing Gas Turbine Fuel Flexibility - GER4601B.

Kohl, A., Nielsen, R., 1997. Gas Purification, Fifth. ed. Gulf Publishing Company, Houston.

Kuramochi, T., Ramírez, A., Turkenburg, W., Faaij, A., 2012. Comparative assessment of CO_2 capture technologies for carbon-intensive industrial processes. Prog. Energy Combust. Sci. 38, 87–112, http://dx.doi.org/10.1016/j.pecs.2011.05.001

Lampert, K., Ziebik, A., 2007. Comparative analysis of energy requirements of CO_2 removal from metallurgical fuel gases. Energy 32, 521–527, http://dx.doi.org/10.1016/j.energy.2006.08.003

Lozza, G., 1990. Bottoming Steam Cycles for combined gas-steam power plants: a theoretical estimation of steam turbine performance and cycle analysis, in: Proceedings of the 1990 ASME Cogen-Turbo. New Orleans, USA. Macchi, E., Consonni, S., Lozza, G., Chiesa, P., 1995. An Assessment of the thermodynamic performance of mixed gas-steam cycles: Part a—intercooled and steam-injected cycles. J. Eng. Gas Turbines Power 117 (3), 489–498.

Manzolini, G., Macchi, E., Binotti, M., Gazzani, M., 2011. Integration of SEWGS for carbon capture in natural gas combined cycle, Part B: reference case comparison. Int. J. Greenh. Gas Control 5, 214–225.

Manzolini, G., Macchi, E., Gazzani, M., 2013a. CO_2 capture in integrated gasification combined cycle with SEWGS—Part B: economic assessment. Fuel 105, 220–227.

Manzolini, G., Macchi, E., Gazzani, M., 2013b. CO_2 capture in natural gas combined cycle with SEWGS, Part B: economic assessment. Int. J. Greenh. Gas Control 12, 502–509.

Manzolini, G., Sanchez Fernandez, E., Rezvani, S., Macchi, E., Goetheer, E.L.V., Vlugt, T.J.H., 2014. Economic assessment of novel amine based CO_2 capture technologies integrated in power plants based on European Benchmarking Task Force methodology. Appl. Energy., http://dx.doi.org/10.1016/j.apenergy.2014.04.066

Meissner III, R.E., Wagner, U., 1983. Low-energy process recovers CO_2. Oil Gas J. 81, 55–58.

Otsuka, H., Tanabe, H., Harada, S., Tanaka, S., Obata, J., Xuewen, C., 2007. Anshan Iron & Steel Group Corporation, China. Construction and operation experience of 300 MW blast furnace gas firing combined cycle power plant. Mitsubishi Heavy Ind.—Tech. Rev 44, 1–6.

Quader, M.A., Ahmed, S., Ghazilla, R.A.R., Ahmed, S., Dahari, M., 2015. A comprehensive review on energy efficient CO_2 breakthrough technologies for sustainable green iron and steel manufacturing. Renew. Sustain. Energy Rev. 50, 594–614, http://dx.doi.org/10.1016/j.rser.2015.05.026

Remus, R., Monsonet, M.A.A., Roudier, S., Sancho, L.D., 2013. Best Available Techniques (BAT) reference document for iron and steel production. JRC Ref. Rep.—Eur. Comm., http://dx.doi.org/10.2791/97469

Romano, M.C., 2013. Ultra-high CO_2 capture efficiency in CFB oxyfuel power plants by calcium looping process for CO_2 recovery from purification units vent gas. Int. J. Greenh. Gas Control 18, 57–67, http://dx.doi.org/10.1016/j.ijggc.2013.07.002

Romano, M.C., Anantharaman, R., Arasto, A., Ozcan, D.C., Ahn, H., Dijkstra, J.W., Carbo, M., Boavida, D., 2013. Application of advanced technologies for CO_2 capture from industrial sources. Energy Procedia 37, 7176–7185, http://dx.doi.org/10.1016/j.egypro.2013.06.655

Romano, M.C., Chiesa, P., Lozza, G., 2010. Pre-combustion CO_2 capture from natural gas power plants, with ATR and MDEA processes. Int. J. Greenh. Gas Control 4, 785–797, http://dx.doi.org/10.1016/j.ijggc.2010.04.015

Tobiesen, A., Hoff, K.A., Haugen, G., Mejdell, T., 2011. Process Evaluations and Simulations of CO_2 apture from Steel Plant Flue gases, in: Industry CCS Workshop. pp. 1–22.

Tsupari, E., Kärki, J., Arasto, A., Pisilä, E., 2013. Post-combustion capture of CO_2 at an integrated steel mill—Part II: economic feasibility. Int. J. Greenh. Gas Control 16, 278–286, http://dx.doi.org/10.1016/j.ijggc.2012.08.017

ULCOS, 2014. ULCOS Project [WWW Document]. URL ⟨http://www.ulcos.org/en/index.php⟩.

Van Selow, E.R., Cobden, P.D., Brink, R.W., Van Den, Hufton, J.R., Wright, A., 2008. Performance of sorption-enhanced water-gas shift as a pre-combustion CO_2 capture technology. Energy Procedia GHGT 9 (1), 689–696.

Van Selow, E.R., Cobden, P.D., Wright, A.D., Van Den Brink, R.W., Jansen, D., 2011. Improved sorbent for the sorption-enhanced water-gas shift process. Energy Procedia 4, 1090–1095, http://dx.doi.org/10.1016/j.egypro.2011.01.159

World Steel Association, 2013. Sustainable Steel Policy and Indicators 2013. World Steel Association, 2014. World Steel in Figures 2014.

Wright, A., White, V., Hufton, J., Selow, E., Van, Hinderink, P., 2008. Reduction in the cost of pre-combustion CO_2 capture through advancements in sorption-enhanced-water–gas-shift. Energy Procedia GHGT 9 (1), 707–714.